Why Has There Been No Global Warming For The Past Decade?

Physics Department Colloquium
UNC Chapel Hill
September 8, 2014

William Happer
Princeton University

Will Happer, Climate Scientist, 1982

GORDON J. MACDONALD
Chief Scientist, The MITRE Corporation, McLean, Virginia

HENRY D.I. ABARBANEL
Staff Scientist, Lawrence Berkeley Laboratories, Berkeley

JOSEPH W. CHAMBERLAIN
Professor of Space Physics and Astronomy, Rice University

FREEMAN J. DYSON
Professor of Physics, Institute for Advanced Studies, Princeton University

HENRY M. FOLEY
Professor of Physics, Columbia University

NORVAL FORTSON
Professor of Physics, University of Washington, Seattle

WILLIAM HAPPER
Professor of Physics, Department of Physics, Princeton University

WALTER H. MUNK
Professor of Geophysics, University of California, San Diego

WILLIAM A. NIERENBERG
Director, Scripps Institution of Oceanography, La Jolla

OSCAR S. ROTHAUS
Professor of Mathematics, Mathematics Department, Cornell University

MALVIN A. RUDERMAN
Centennial Professor of Physics, Columbia University

SAM B. TREIMAN
Eugene Higgins Professor of Physics, Princeton University

JOHN VESECKY
Center for Radar Astronomy, Stanford University

FREDRIK ZACHARIASEN
Professor of Theoretical Physics, California Institute of Technology

THE LONG-TERM IMPACTS OF INCREASING ATMOSPHERIC CARBON DIOXIDE LEVELS

Edited by
GORDON J. MACDONALD

BALLINGER PUBLISHING COMPANY
Cambridge, Massachusetts
A Subsidiary of Harper & Row, Publishers, Inc.

What is all the fuss about?

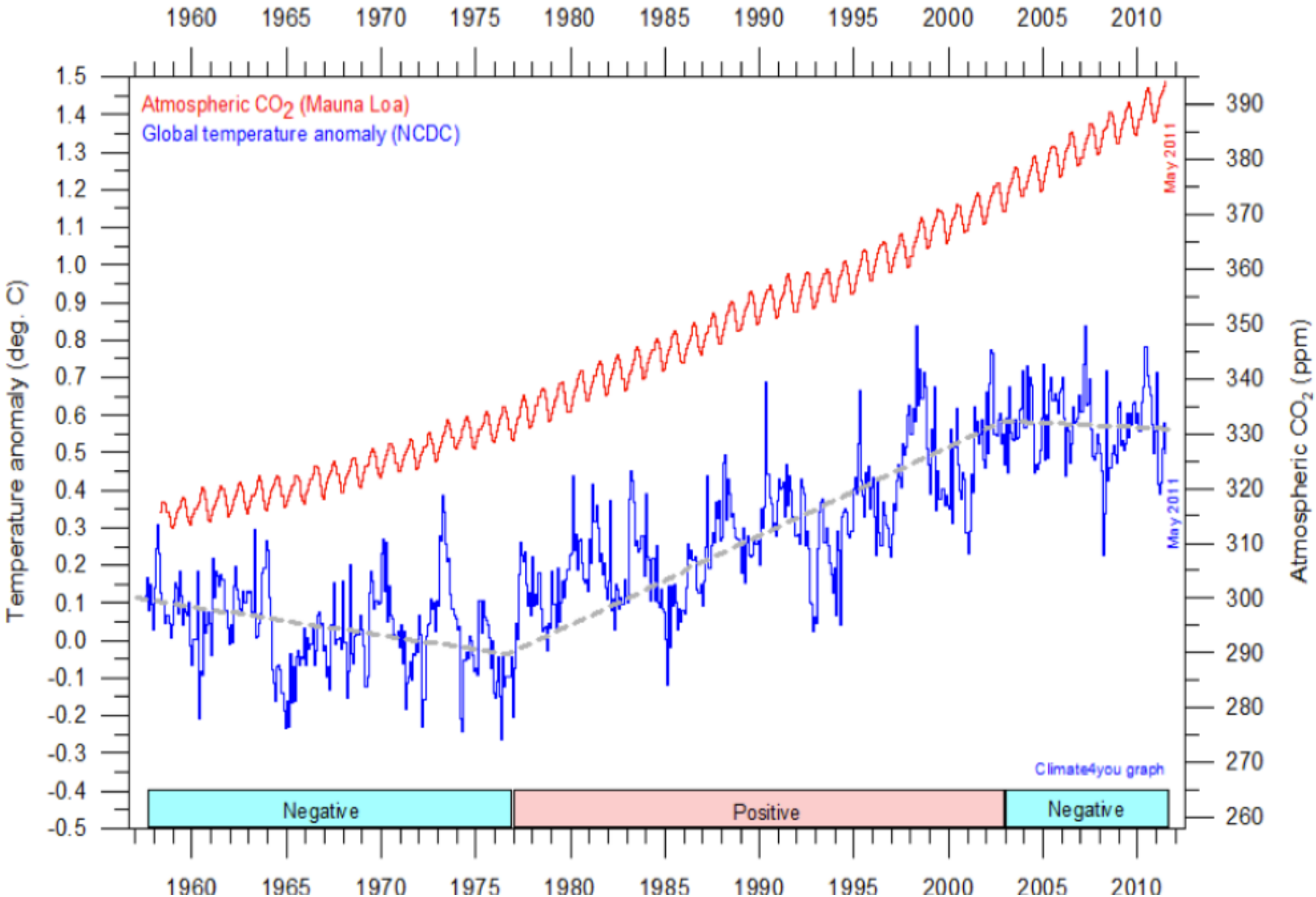

Climate Models Don't Work; Red is Observed; Bars are Models

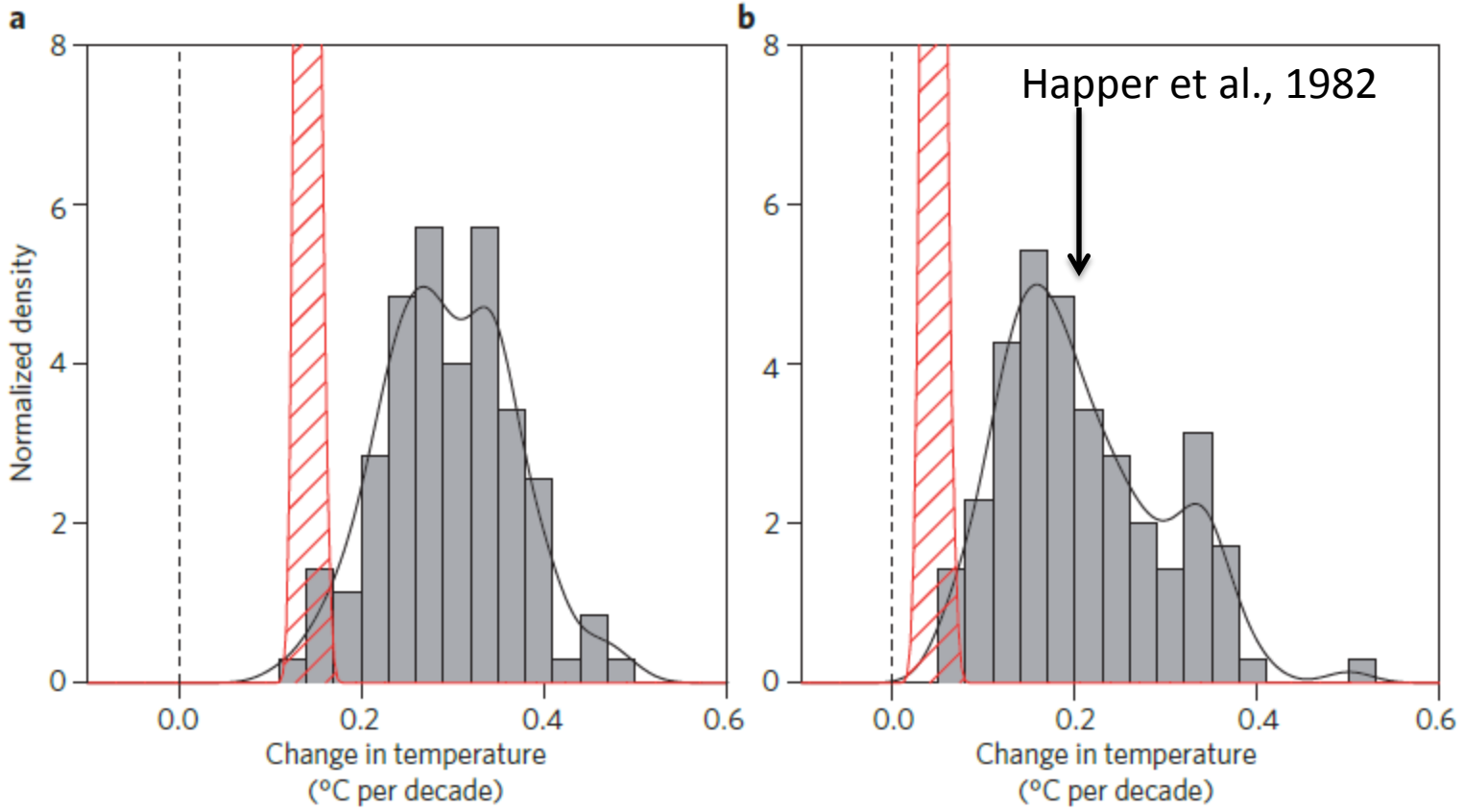

Figure 1 | Trends in global mean surface temperature. **a**, 1993–2012. **b**, 1998–2012. Histograms of observed trends (red hatching) are from 100 reconstructions of the HadCRUT4 dataset[1]. Histograms of model trends (grey bars) are based on 117 simulations of the models, and black curves are smoothed versions of the model trends. The ranges of observed trends reflect observational uncertainty, whereas the ranges of model trends reflect forcing uncertainty, as well as differences in individual model responses to external forcings and uncertainty arising from internal climate variability.

Nature Climate Change, Vol 3, p. 767, September 2013.

Der Spiegel, Jan. 2013

The press is beginning to notice!

Klimawandel: Forscher rätseln über Stillstand bei Erderwärmung

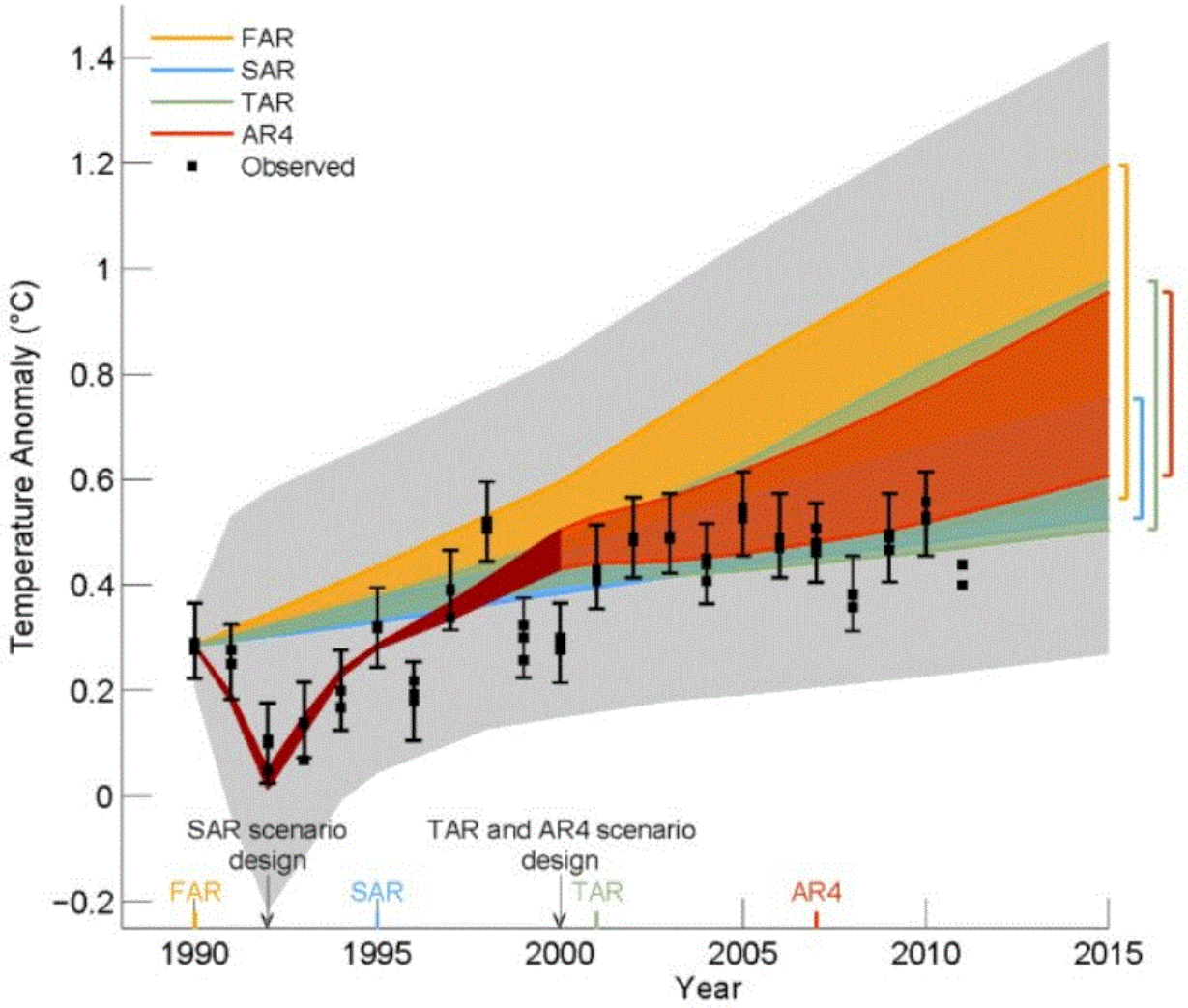

IPCC WGI Fifth Assessment Report (Draft)

Satellite temperature measurements of lower atmosphere show little warming

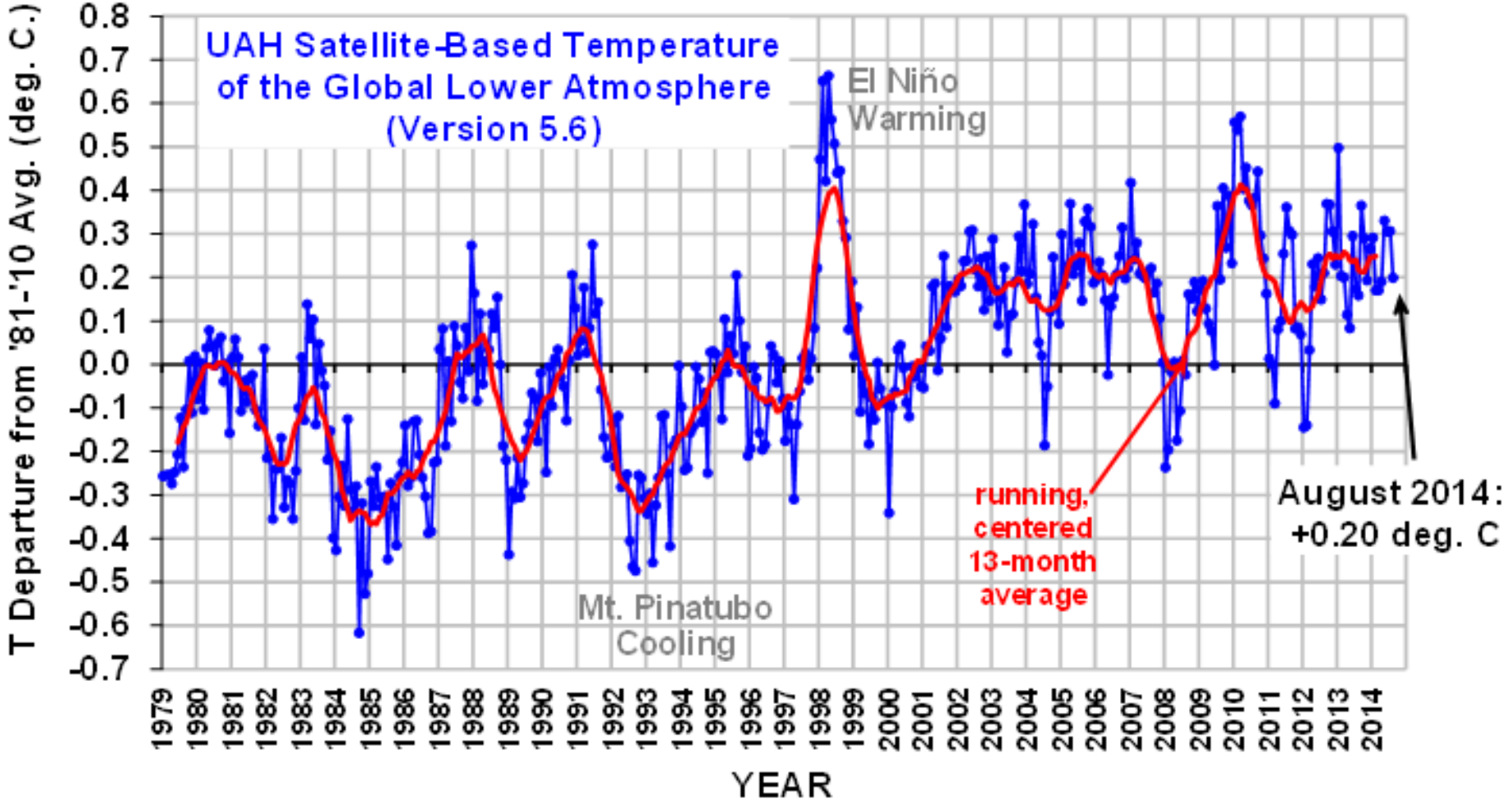

http://www.drroyspencer.com/latest-global-temperatures/

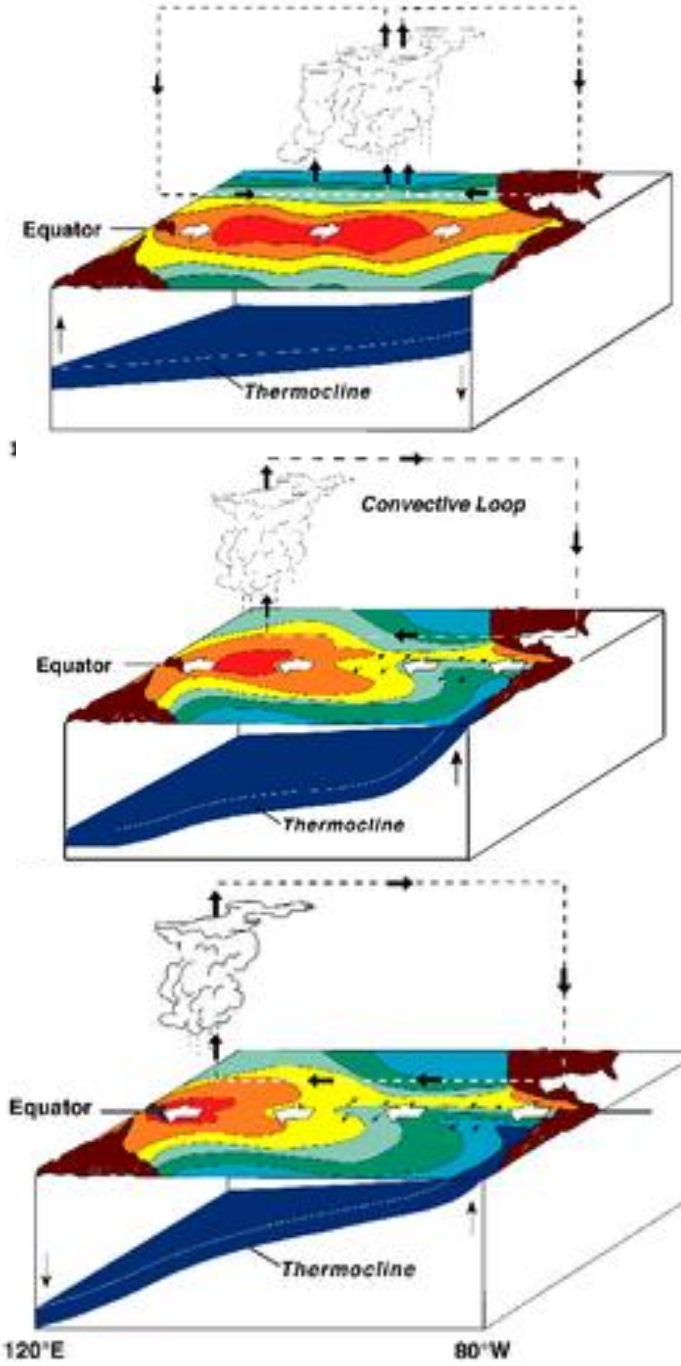

El Nino

Normal

La Nina

Al Gore, Climate Scientist, Nobel Laureate.

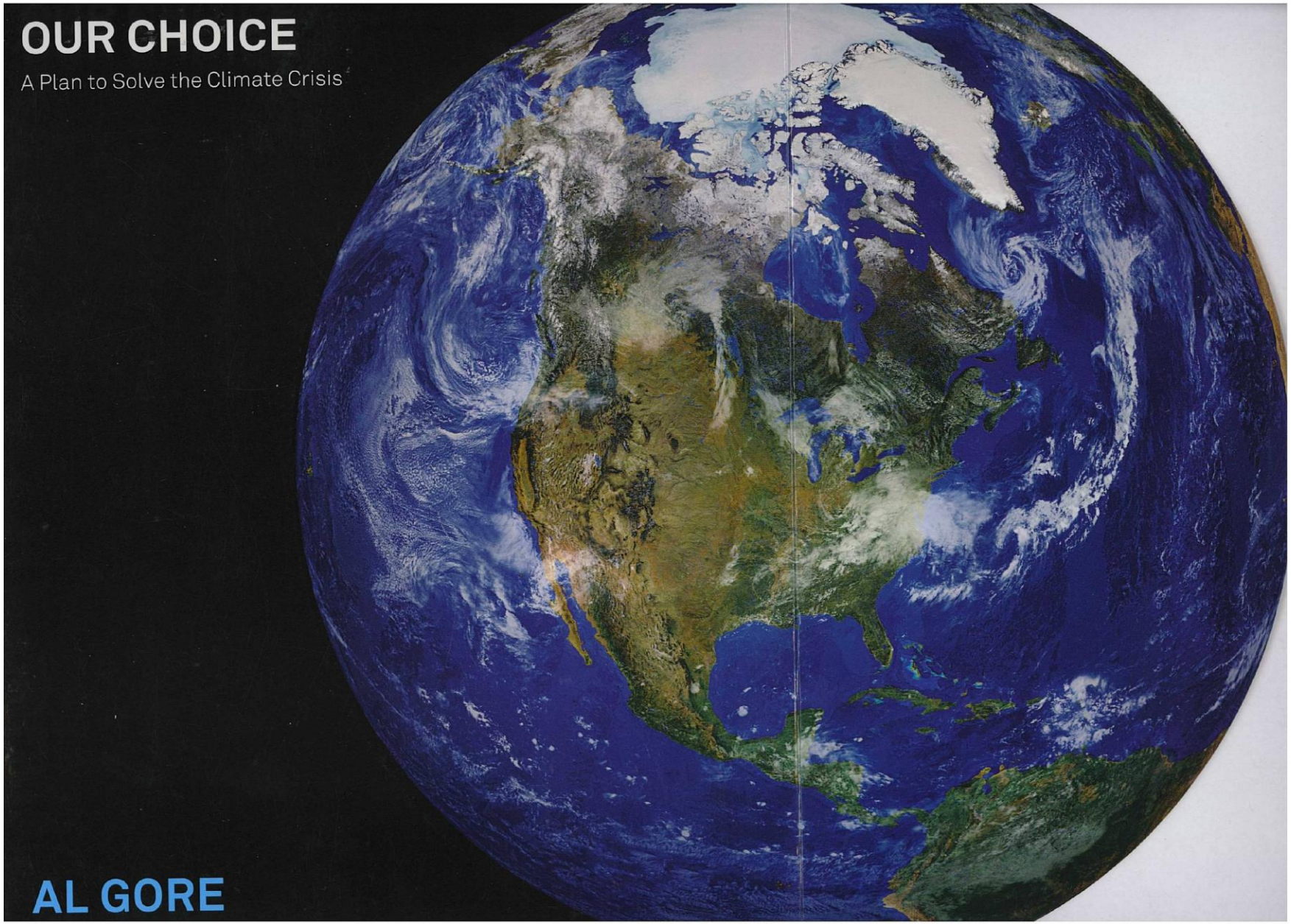

The Original for the Image on the Book's Cover.

The Image on the Inner Cover Showing the Lamentable Effects of More CO2

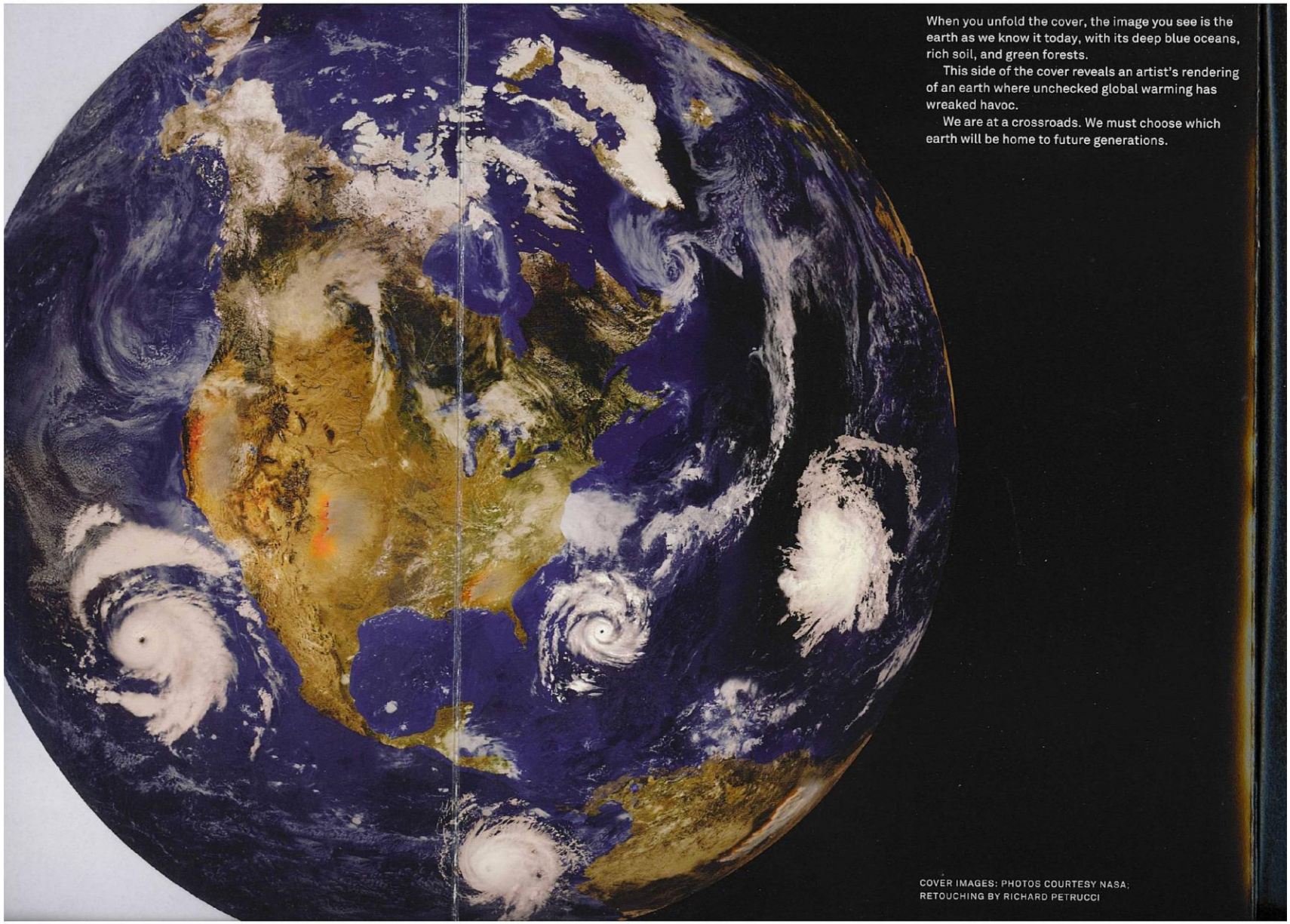

Hurricane (Tropical Cyclone) Tracks; 1985-2005; (Wikipedia)

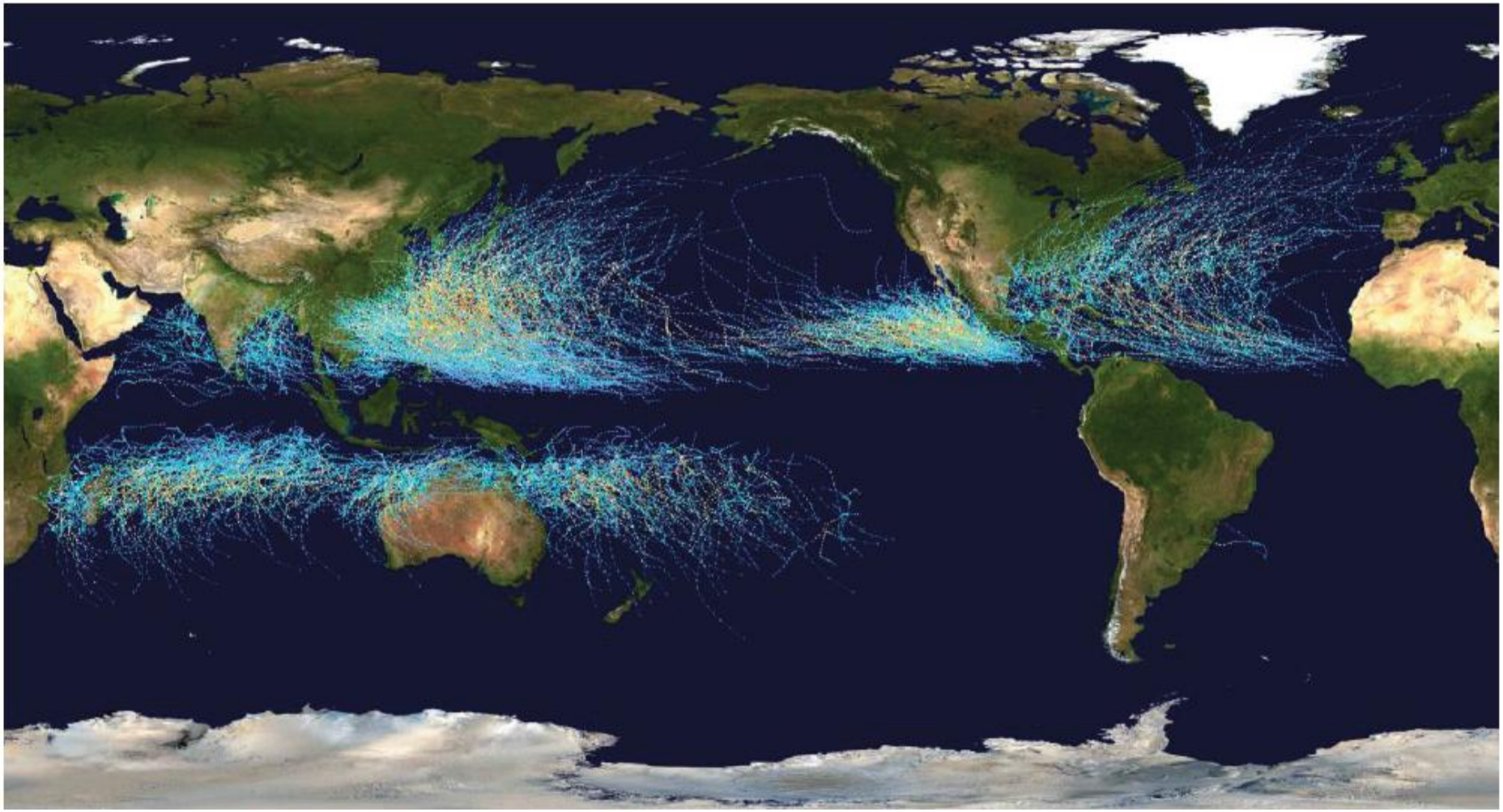

No Coriolis force at equator → No hurricanes

Low clouds spiral in counterclockwise in North; clockwise in South

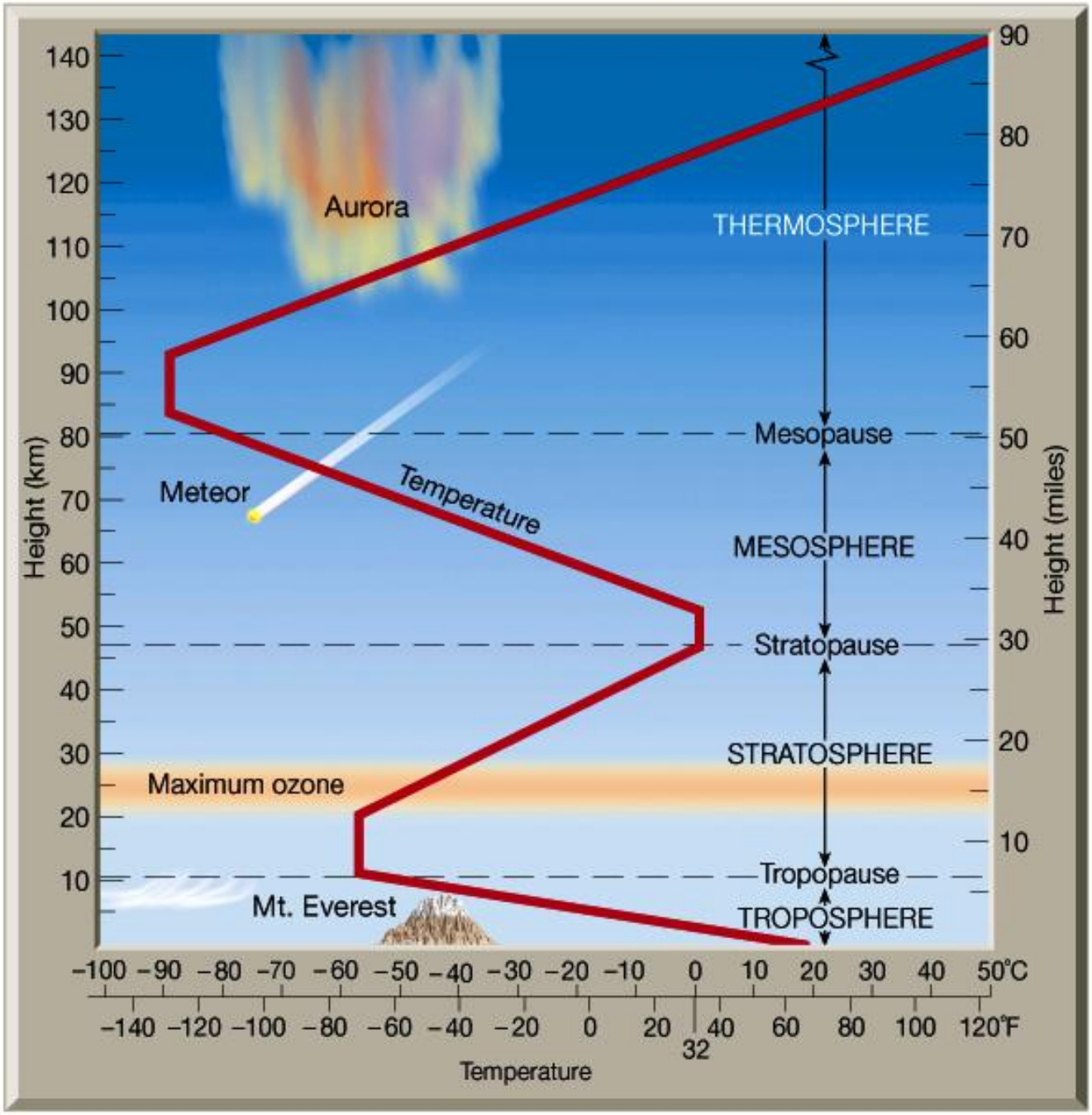
Aurora
THERMOSPHERE
Mesopause
Meteor
Temperature
MESOSPHERE
Stratopause
STRATOSPHERE
Maximum ozone
Tropopause
Mt. Everest
TROPOSPHERE
Height (km)
Height (miles)
140
130
120
110
100
90
80
70
60
50
40
30
20
10
90
80
70
60
50
40
30
20
10
−100 −90 −80 −70 −60 −50 −40 −30 −20 −10 0 10 20 30 40 50°C
−140 −120 −100 −80 −60 −40 −20 0 20 32 40 60 80 100 120°F
Temperature

Atmospheric Circulation

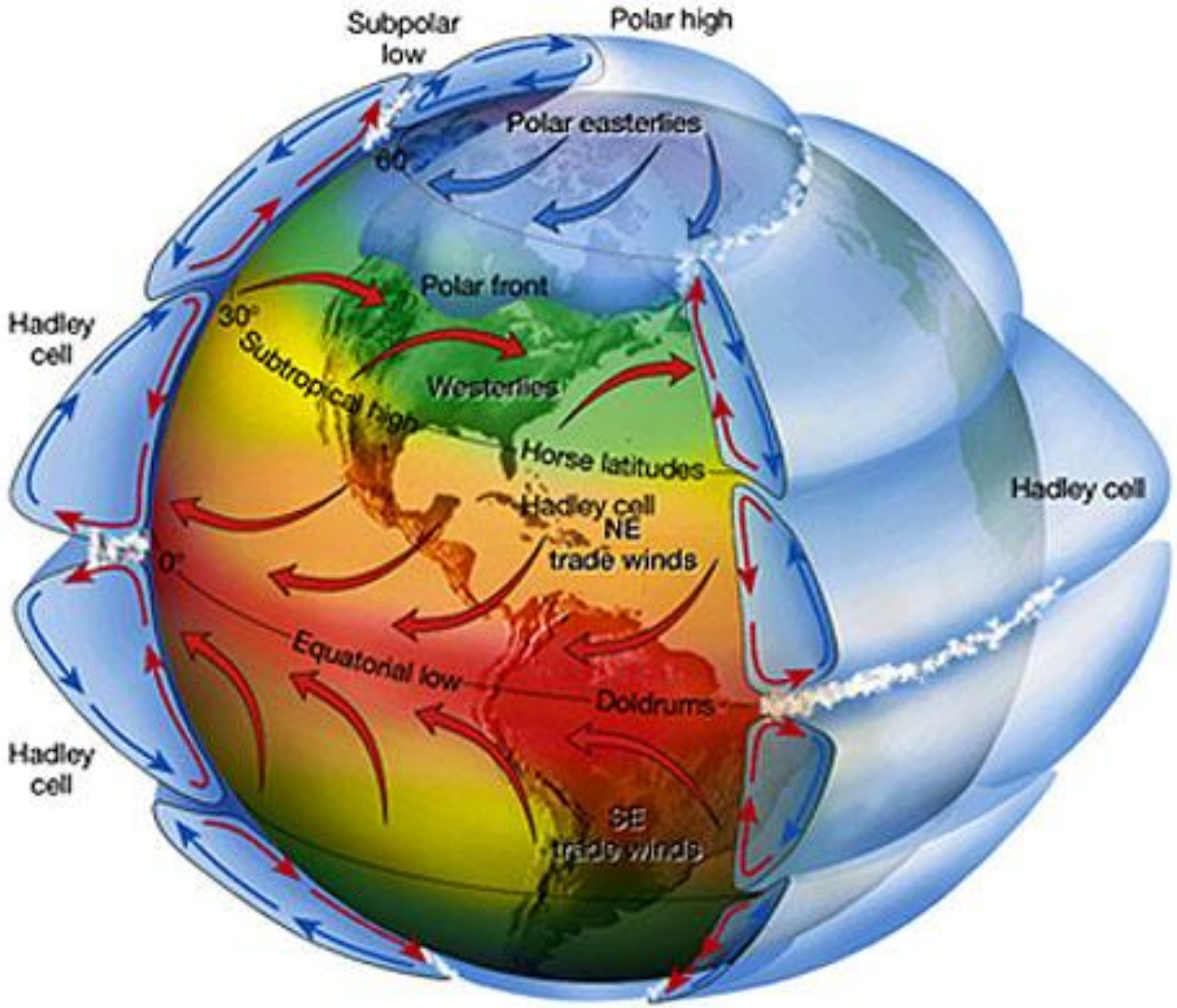

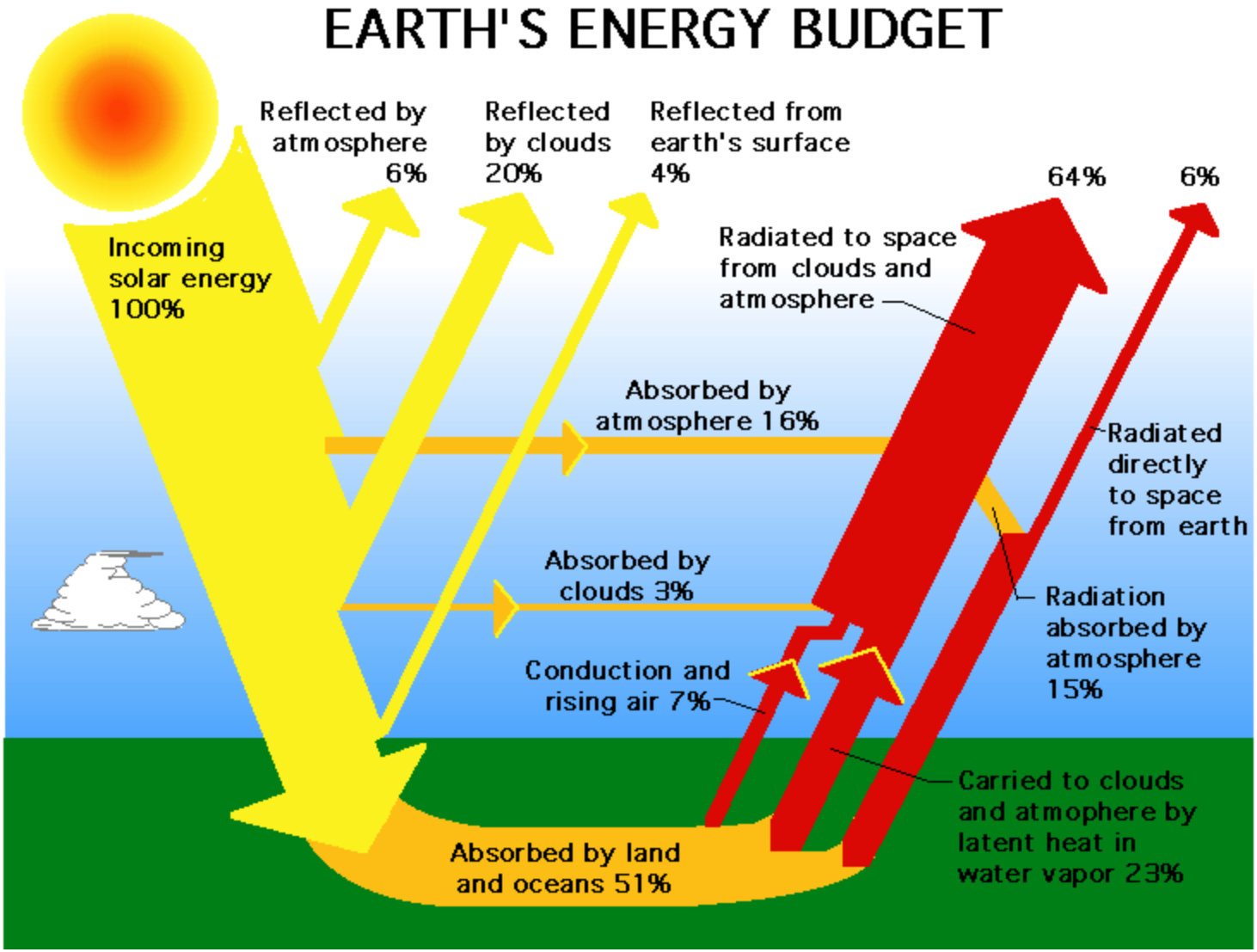

A NASA Website

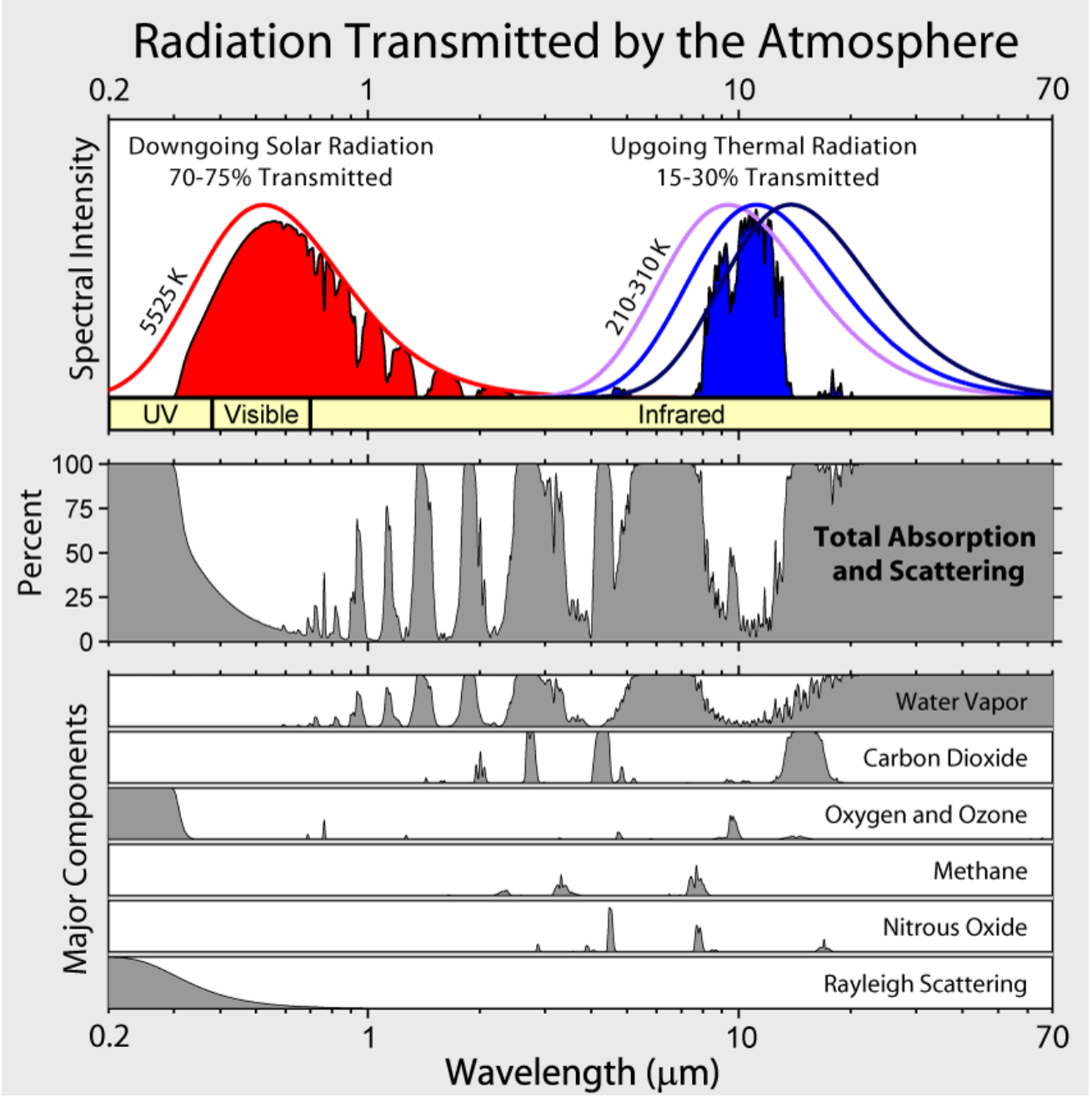
Radiation Transmitted by the Atmosphere
0.2
1
10
70
Spectral Intensity
Downgoing Solar Radiation
70-75% Transmitted
Upgoing Thermal Radiation
15-30% Transmitted
5525 K
210-310 K
UV
Visible
Infrared
Percent
100
75
50
25
0
Total Absorption and Scattering
Major Components
Water Vapor
Carbon Dioxide
Oxygen and Ozone
Methane
Nitrous Oxide
Rayleigh Scattering
0.2
1
10
70
Wavelength (μm)

Examples of FTIR Data from a Satellite

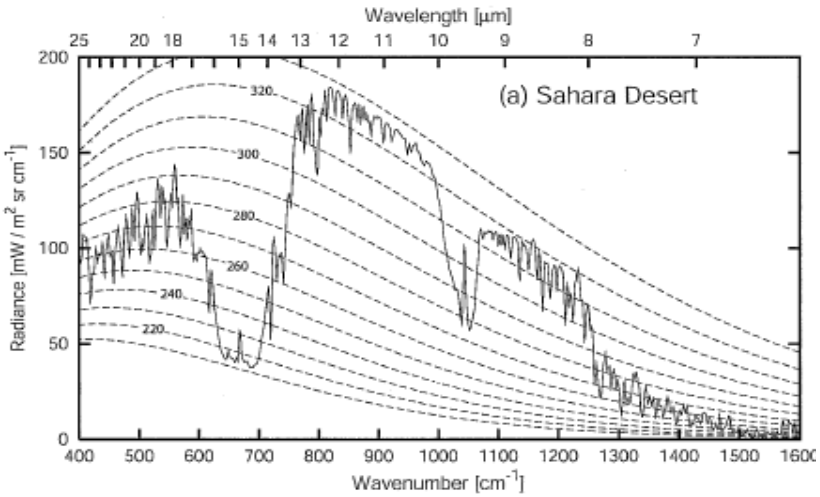

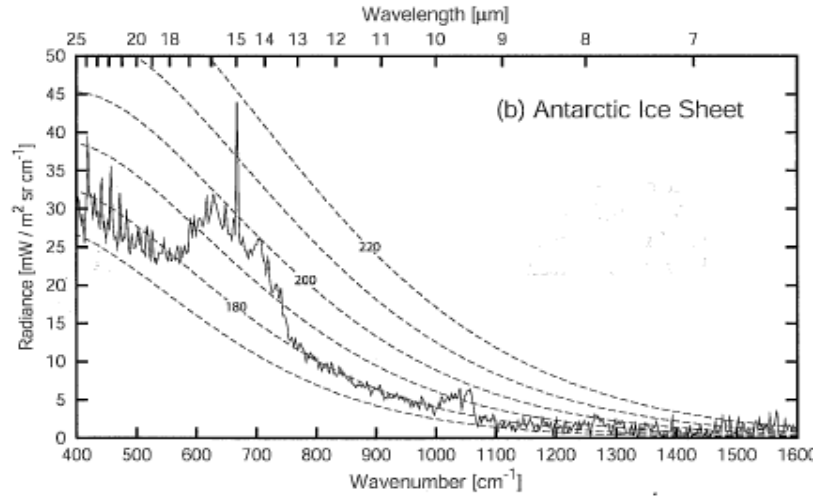

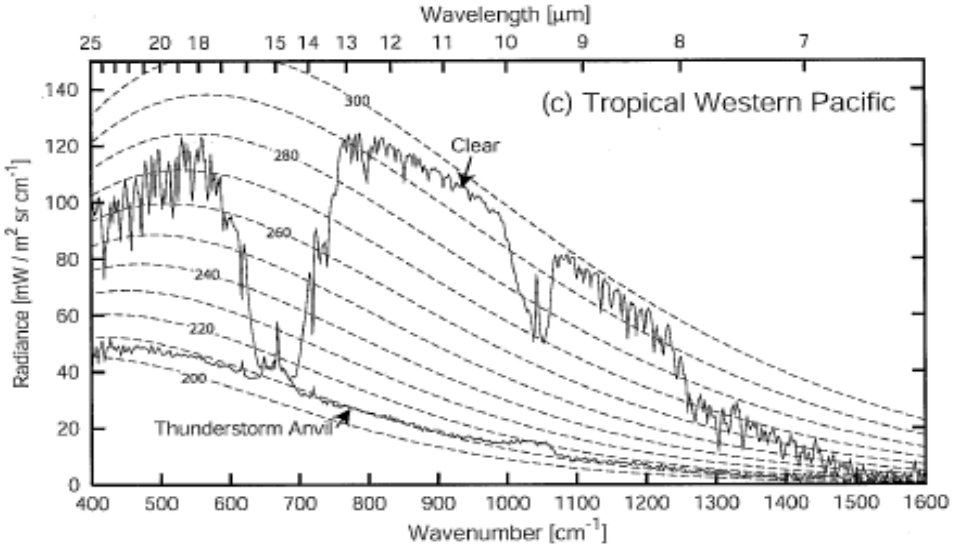

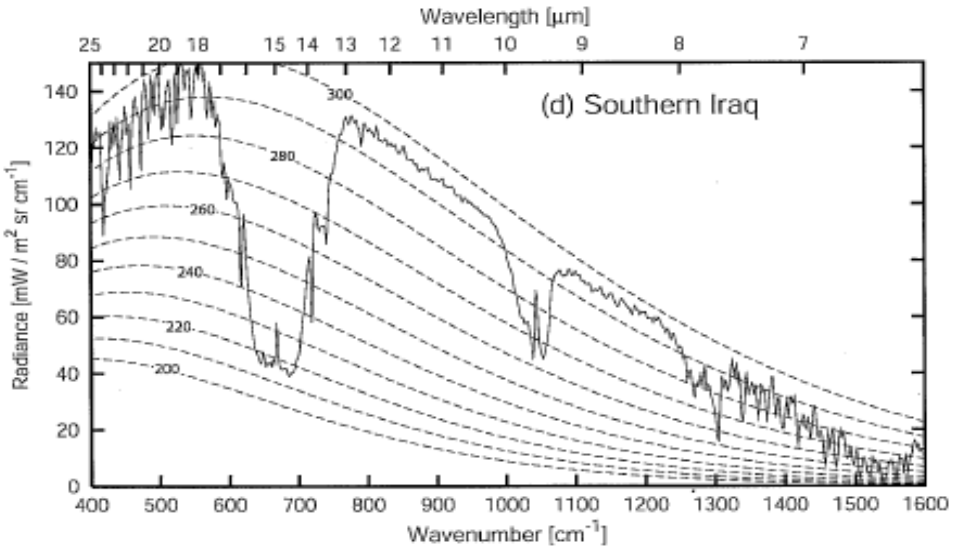

Fig. 8.3: Examples of moderate resolution IR spectra observed by a satellite spe
trometer. Except for the curve labeled "thunderstorm anvil" in panel (c), all spect
were obtained under cloud-free conditions. *(Nimbus-4 IRIS data courtesy of the Go*
dard EOS Distributed Active Archive Center (DAAC) and instrument team leader I
Rudolf A. Hanel.)

One Slide Summary of Global Warming Theory
Key Parameters: forcing ΔQ_2 and feedback f

Steady-State Temperature Change for Doubled CO2

$$\Delta T = \frac{T_e \Delta Q_2}{4 Q_e (1-f)} = \frac{0.30\,\Delta Q_2}{1-f}\ \mathrm{K\ m^2\ W^{-1}} = 3.4\ \mathrm{K} = \frac{1.1\ \mathrm{K}}{(1-2/3)}.$$

$Q_e = (1-\alpha_e)F_e/4 = \sigma \epsilon_e T_e^4 = 236\ \mathrm{W\ m^{-2}}$ = mean radiation of earth to space.

$\alpha_e = 0.306$ albedo (mostly clouds).

$F_e = 1361\ \mathrm{W\ m^{-2}}$ = mean solar flux at earth's orbit.

$T_e = 288\ \mathrm{K}$ = mean surface temperature of Earth.

$\epsilon_e = 0.606$ = effective (contrived) emissivity of Earth for T_e.

$f = 0.25\,T_e\ \partial \ln(1-\alpha_e)/\partial T - T_e\ \partial \ln \epsilon_e/\partial T = 2/3$ (per IPCC) = feedback.

$\Delta Q_2 = 3.7\ \mathrm{W\ m^{-2}}$ (per IPCC) = radiative forcing for doubled CO2.

IPCC values of f and ΔQ_2 give far (at least a factor of 3) too much warming.
Both probably wrong in a way that exaggerates warming!

The Villain!

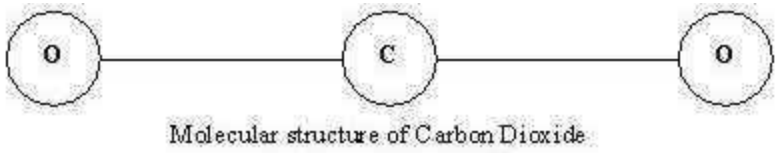

Molecular structure of Carbon Dioxide

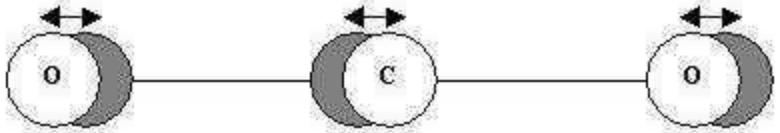

The asymmetric stretch mode

2349 cm $^{-1}$
frequency too high for greenhouse warming

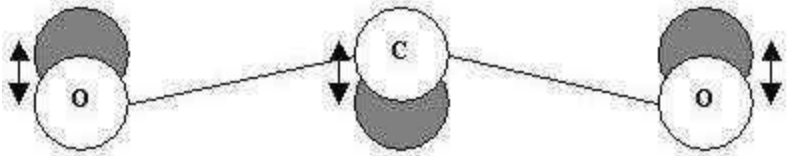

The bending mode

666 cm $^{-1}$ (Satan's number)
greenhouse warming

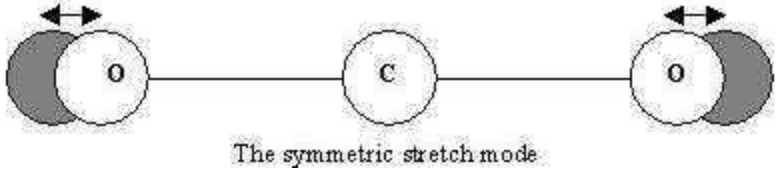

The symmetric stretch mode

1388 cm^{-1}
no changing dipole moment,
no absorption or emission

Fermi Resonances

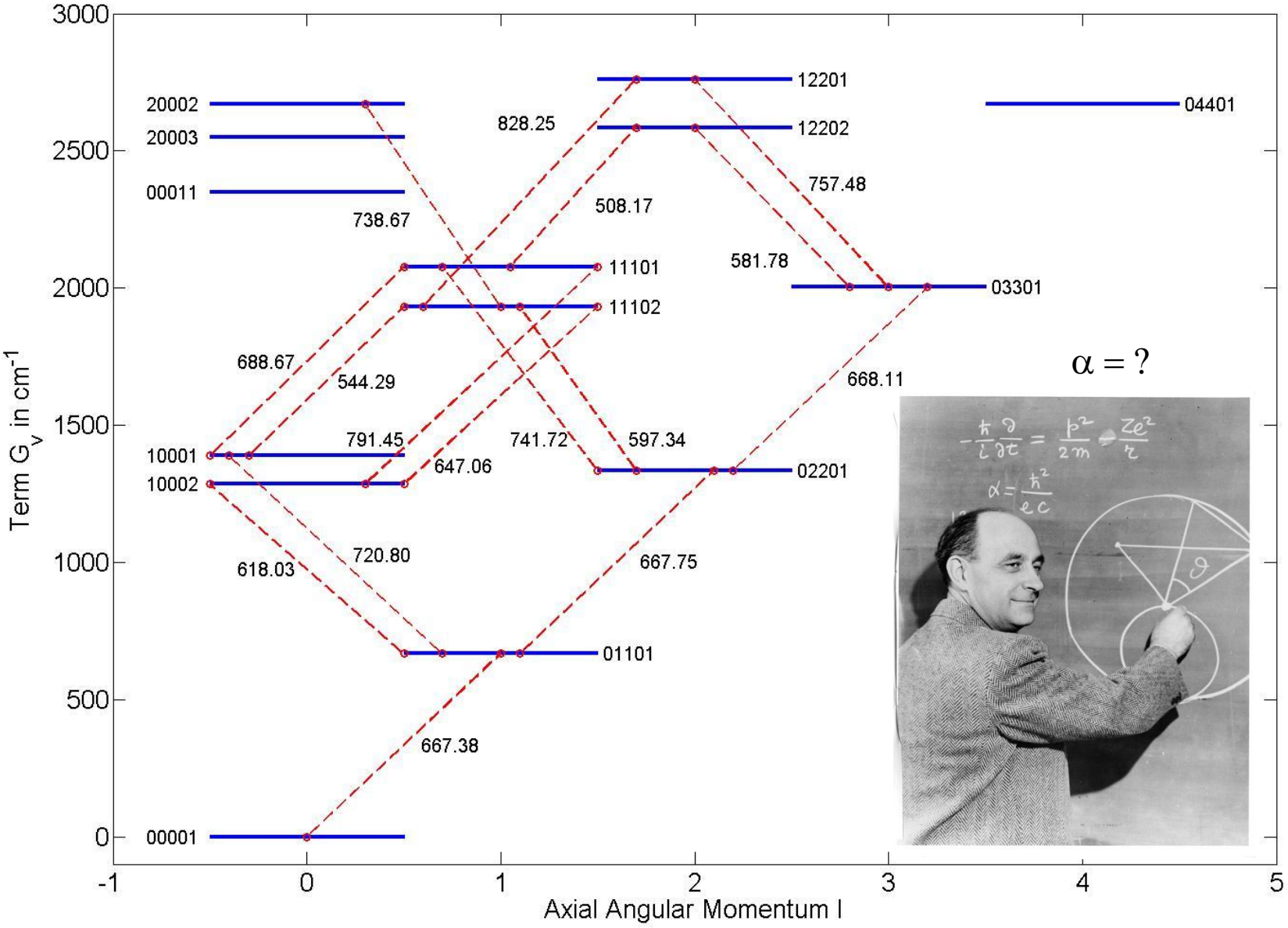

What is wrong with this slide?

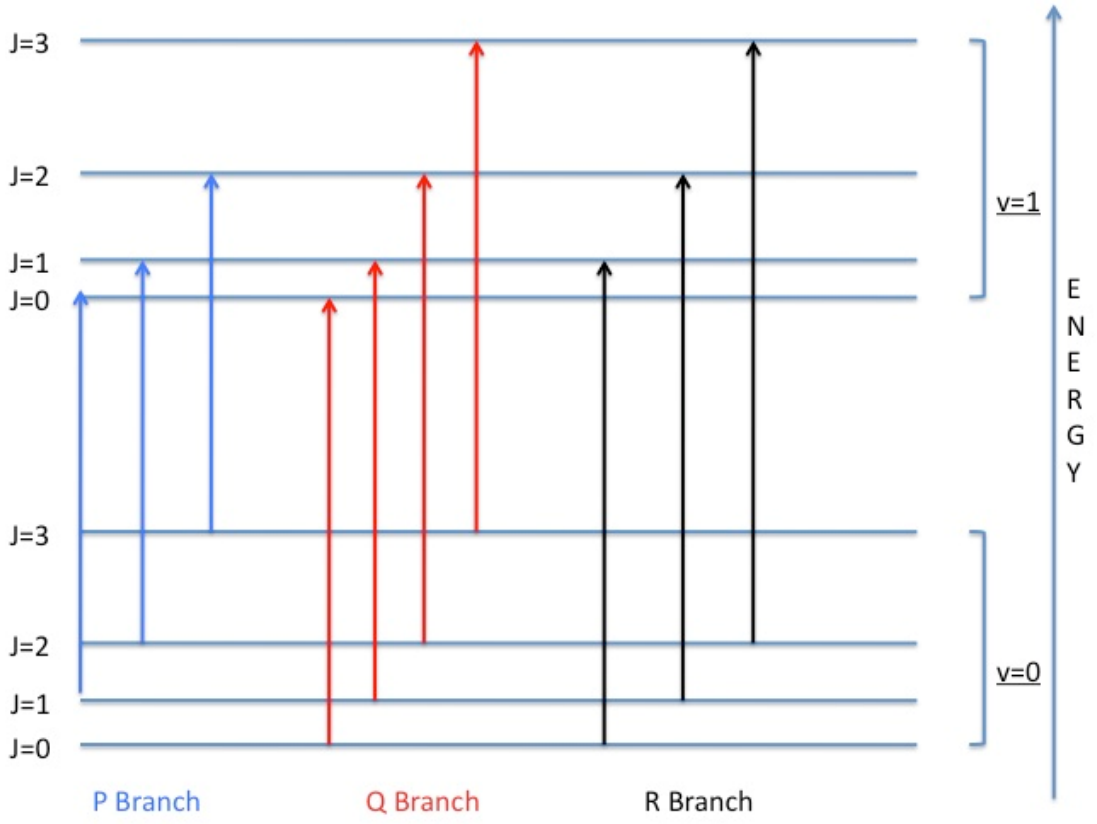

Fig. 6 Schematic diagram of P, Q, and R branch transitions

Attenuation Coefficient (e-foldings / length)

$$\kappa = N \sum_{eg} \sigma_{eg} = N \sum_{eg} S_{eg} G_{eg}$$

Line shape

N is the number density of CO_2 molecules, and σ_{eg} is the cross section of the transition from a lower state g to an upper state e; G_{eg} is the lineshape function.

Line strength (in cm)

$$S_{eg} = \frac{8\pi^3 \nu_{eg} |D_{eg}|^2 e^{-E_g/kT} \left(1 - e^{-hc\nu_{eg}/kT}\right)}{hcZ}$$

ν_{eg} = frequency (in cm^{-1}) of the transition, D_{eg} = the electric dipole matrix element, E_g = lower-state energy, T = absolute temperature, k = Boltzmann's constant, h = Planck's constant, c = speed of light, T = absolute temperature.

Partition function

$$Z = \sum_j e^{-E_j/kT}$$

Normalized line shapes

$$\int_0^\infty G_{eg} d\nu = 1$$

A Lorentzian line shape

$$G_{eg} = \frac{\mu_{eg}/\pi}{\mu_{eg}^2 + (\nu - \nu_{eg})^2}$$

μ_{eg} = broadening; ν = frequency; ν_{eg} = resonance.

A Voigt line shape

$$G_{eg} = \frac{\mu_{eg}}{\pi}\sqrt{\frac{m}{2\pi kT}}\int_{-\infty}^{\infty} \frac{e^{-mv^2/2kT}\,dv}{\mu_{eg}^2 + (\nu - \nu_{eg}[1 + v/c])^2}$$

Neither Lorentzian nor Voigt line shapes are correct in the far wings!

Thousands of lines! Linestrengths vary by 10 orders of magnitude.

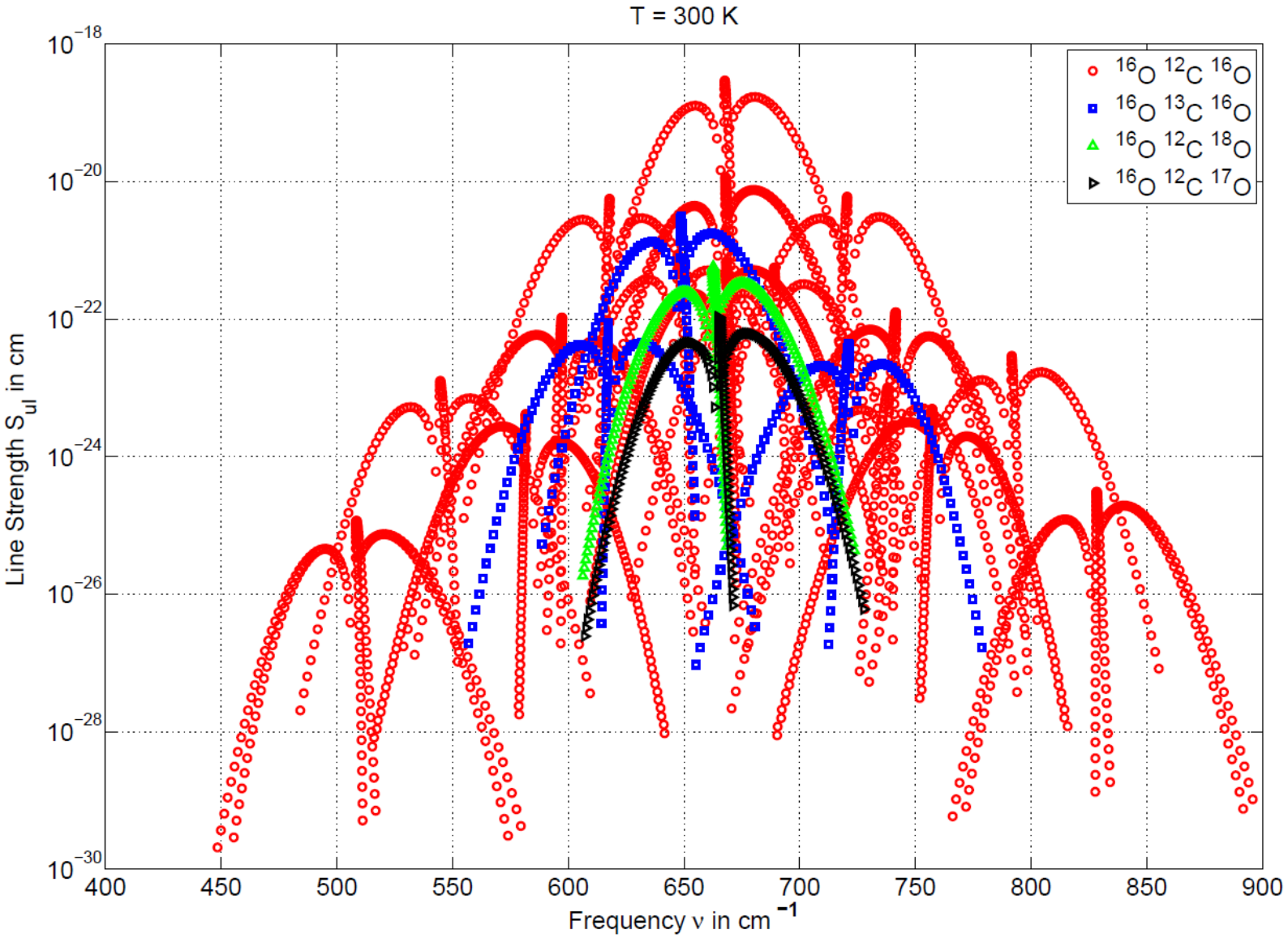

Very Slow Partial Radiative Decay Rates of CO2 Molecules

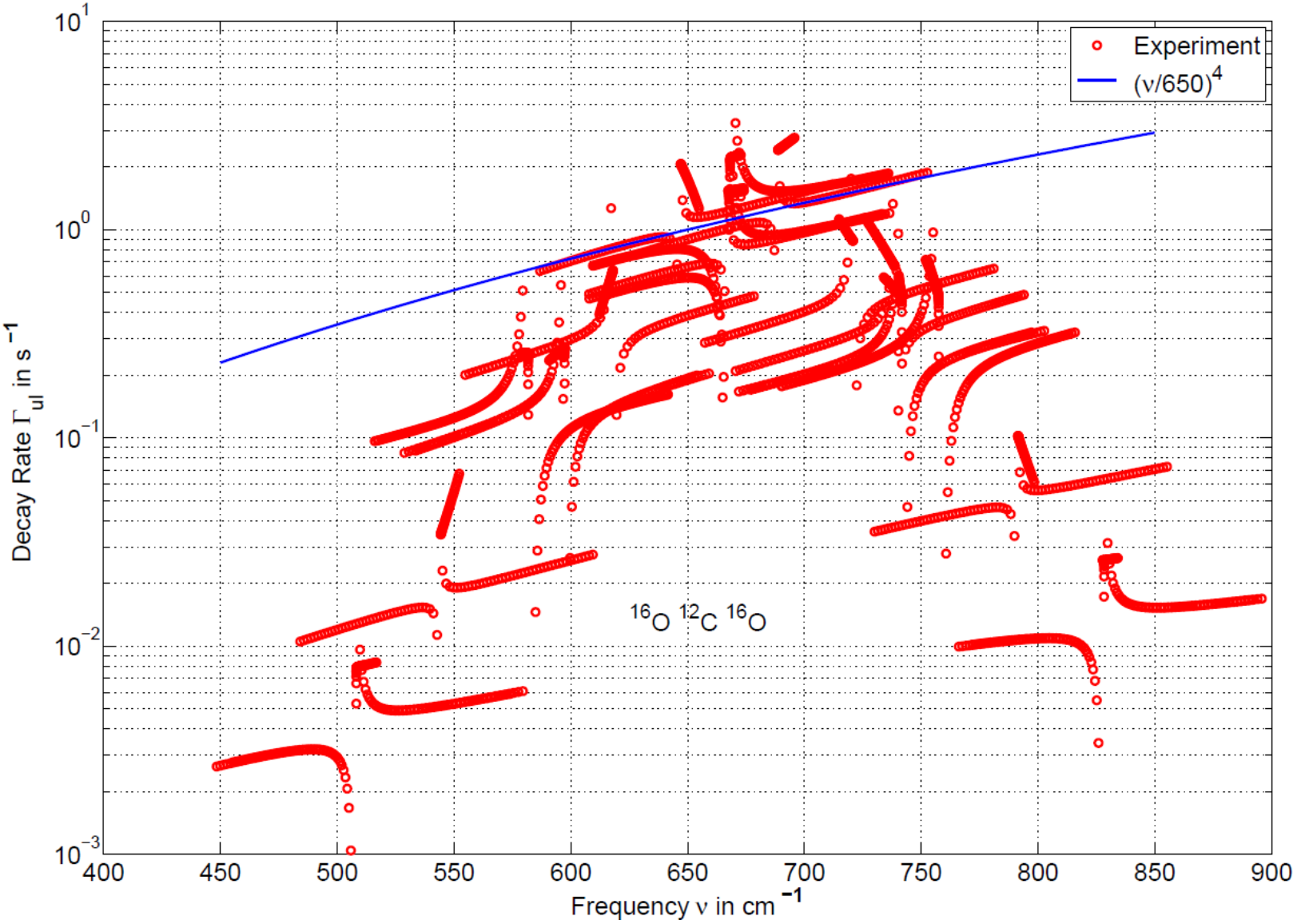

Less pressure broadening of cross sections at high altitude. Q-branch lines.

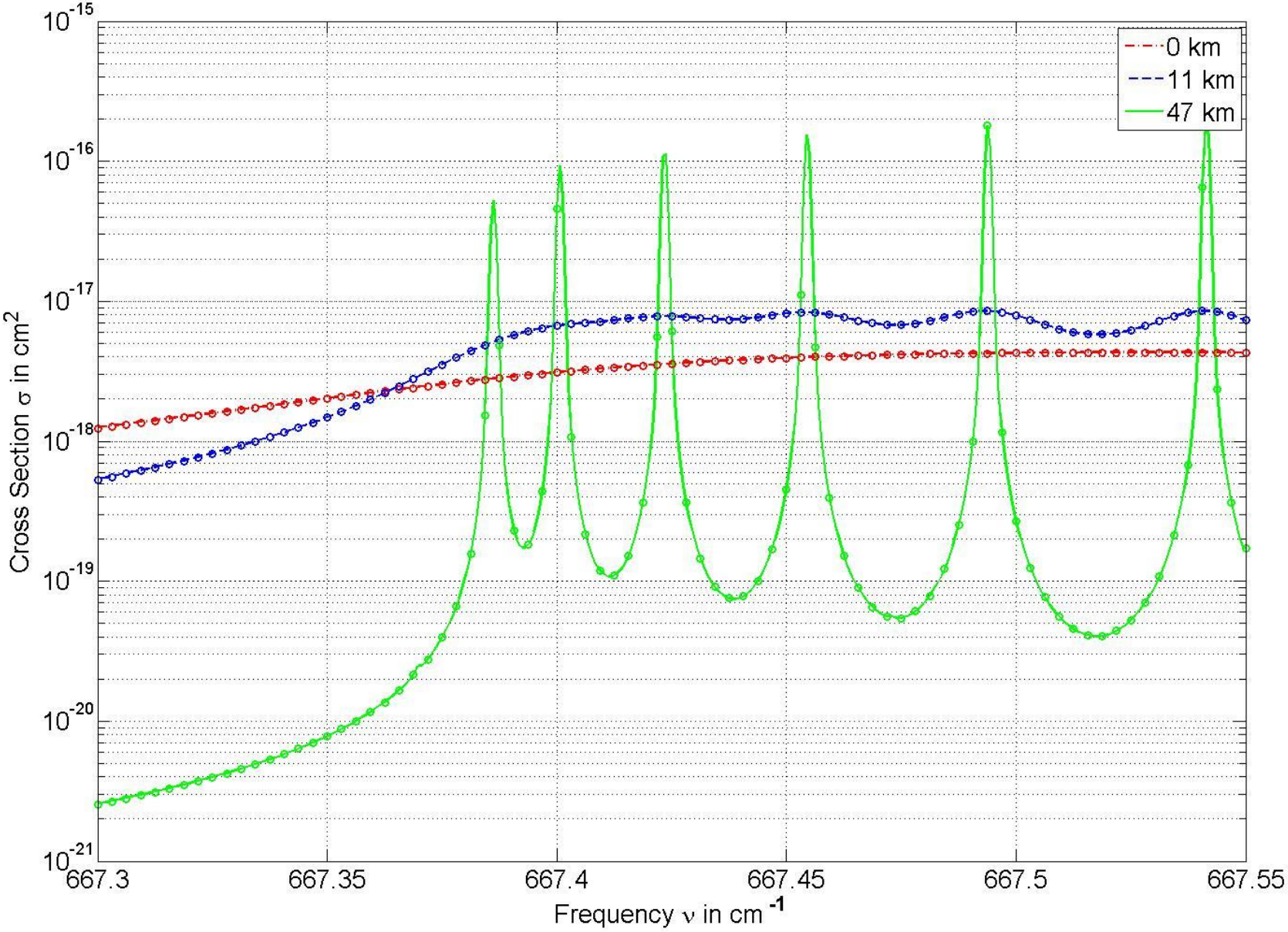

Schwartzschild-Milne Equation: Downwelling Flux at the Surface

$$J(0) = \int_0^\infty \kappa(z) B(z) e^{-\rho(z)} dz$$

K. Schwartzschild

E. A. Milne

Optical Depth from Surface to Altitude z

$$\rho(z) = \int_0^z \kappa(z') dz'$$

Planck Brightness

$$B = \frac{2hc^2\nu^3}{e^x - 1}, \quad \text{where} \quad x = \frac{hc\nu}{kT}$$

M. Planck

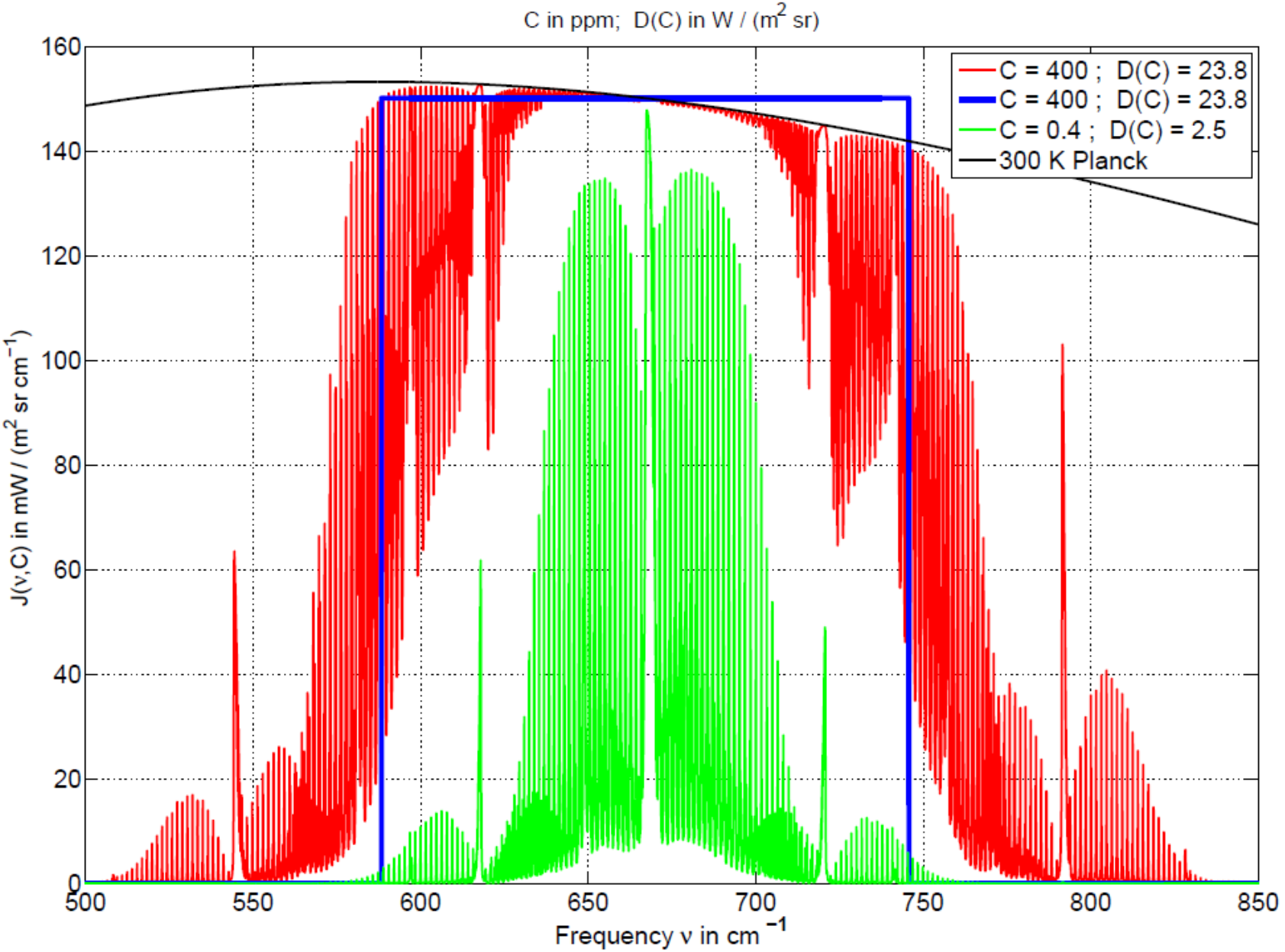
C in ppm; D(C) in W / (m2 sr)
C = 400 ; D(C) = 23.8
C = 400 ; D(C) = 23.8
C = 0.4 ; D(C) = 2.5
300 K Planck
J(ν,C) in mW / (m2 sr cm−1)
Frequency ν in cm −1
0
20
40
60
80
100
120
140
160
500
550
600
650
700
750
800
850

Logarithmic dependence of down-welling IR on CO_2 concentration.

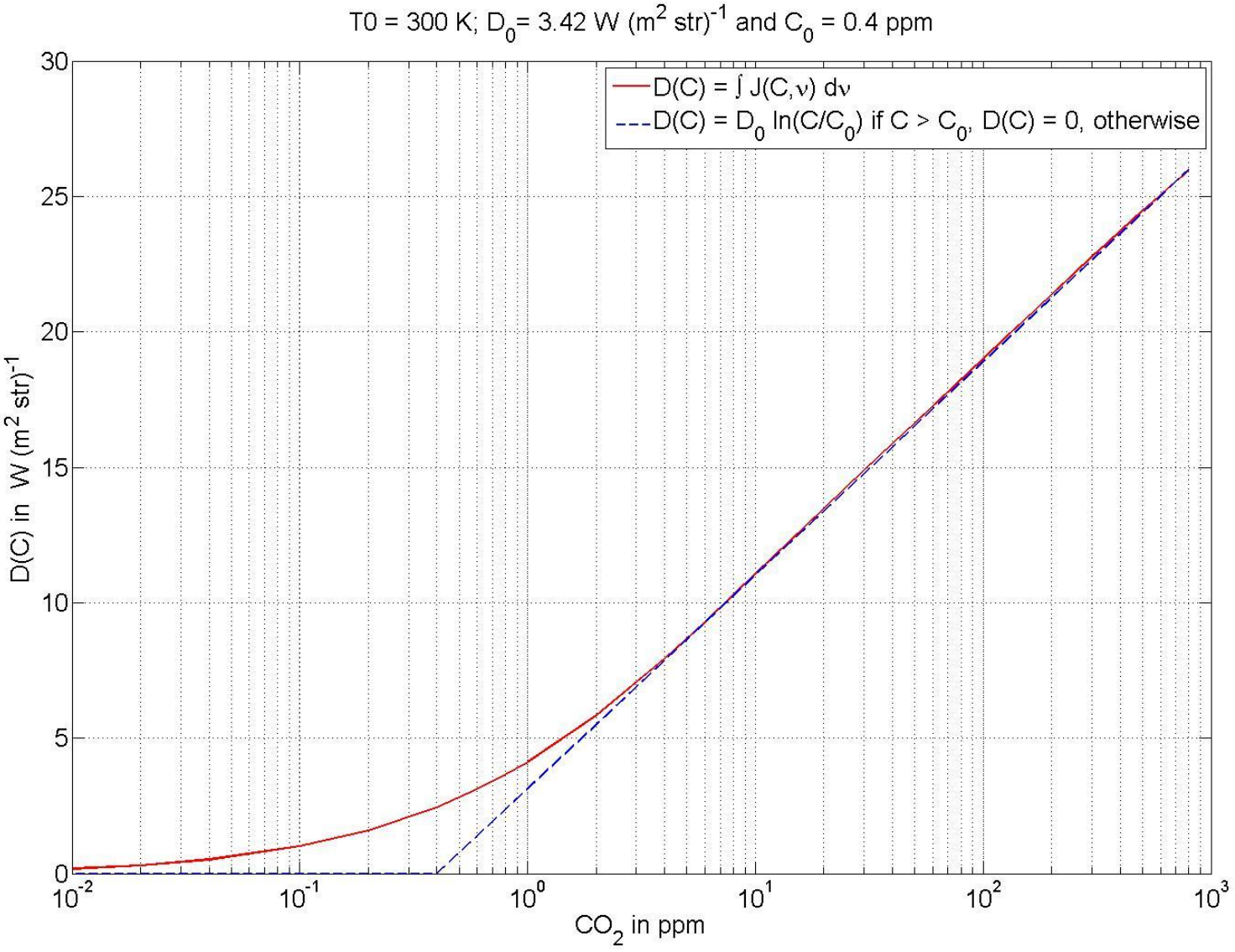

Logarithmic Dependence of Warming on CO_2 Concentration

Svante Arrhenius
Worlds in the Making, The Evolution of the Universe
(page 53)

"If the quantity of carbon dioxide in the air should sink to one half its present percentage, the temperature would fall by 4 K; a diminution by one-quarter would reduce the temperature by 8 K. On the other hand any doubling of the percentage of Carbon dioxide in the air would raise the temperature of the Earth's surface by 4 K, and if the carbon dioxide were increased four fold, the temperature would rise by 8 K."

$$\begin{aligned} \Delta T &= \frac{S}{\ln(2)} \ln(C/C_0), \quad \text{for} \quad C > C_0 \\ &= 0, \quad \text{otherwise.} \end{aligned}$$

C = CO_2 concentration; C_0 = saturation concentration; S = Doubling Sensitivity

The doubling sensitivity S for greenhouse warming by CO_2 is poorly known. IPCC claims S = 1.5 K to 4.5 K.

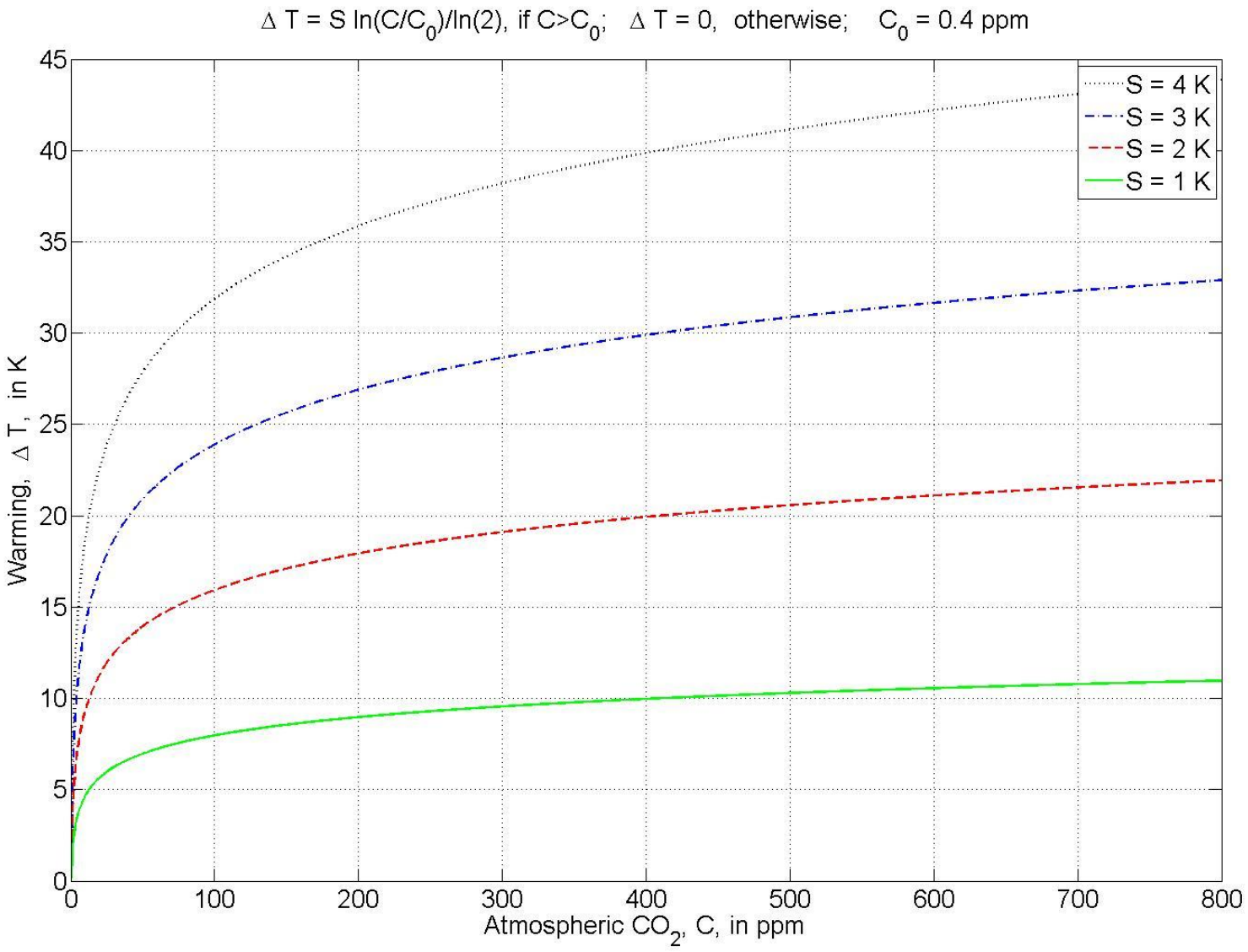

Triangular Approximation to CO2 Cross Section Give Logarithmic Warming

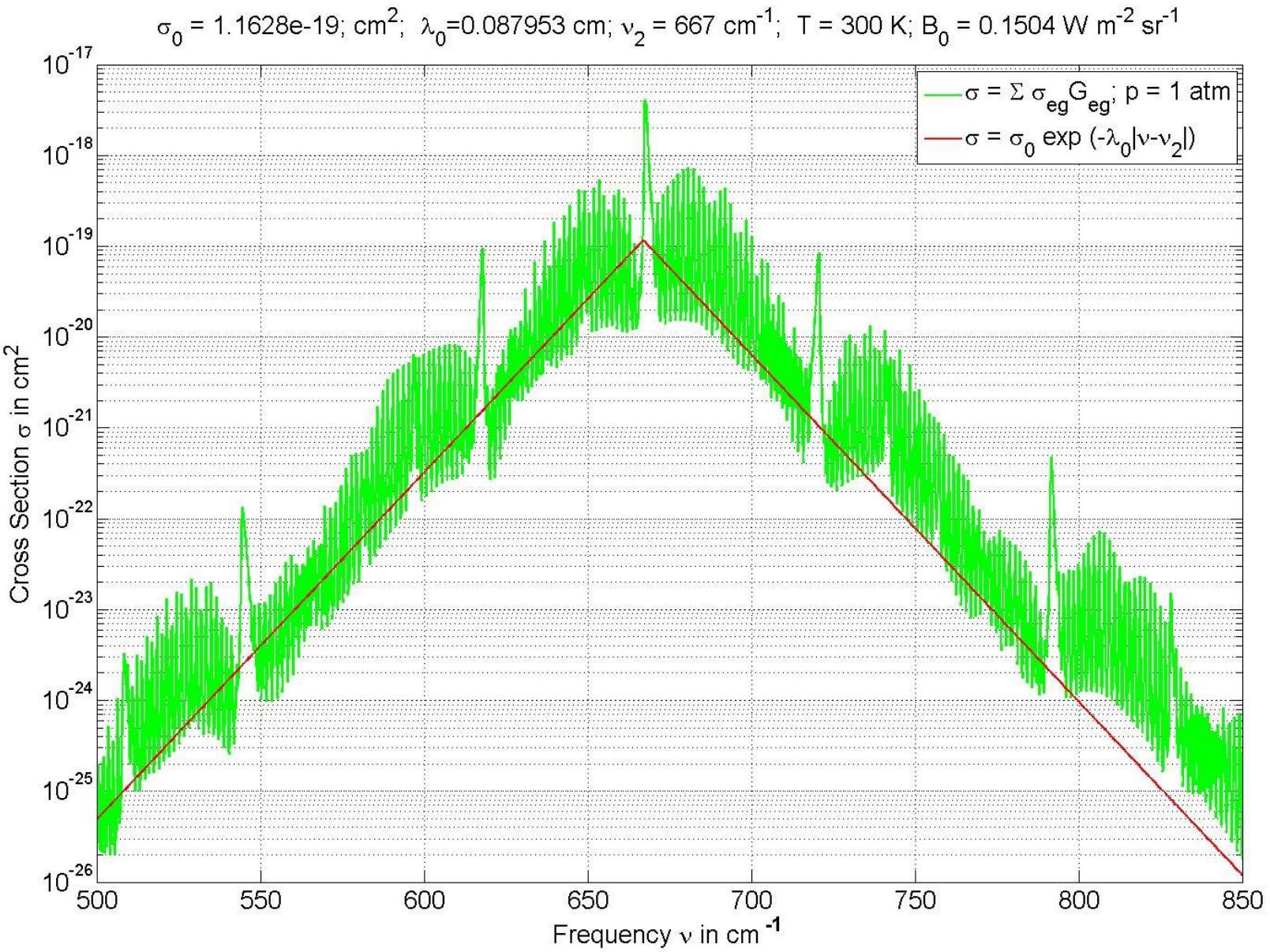

LOGARITHMIC RESPONSE TO CO2 COLUMN DENSITY N

Surface back-radiation from CO2 is very nearly blackbody at surface temperature T_e between upper and lower band limits $\nu_\pm$. Multiplying by π for solid angle we find:

$$Q = \pi \int_{\nu_-}^{\nu_+} B(\nu) d\nu \approx \pi(\nu_+ - \nu_-) B_0, \quad \text{with} \quad B_0 = B(\nu_0).$$

Band-edge frequencies $\nu_\pm$ are where optical depth to space =1.

$$N\sigma(\nu_\pm) = 1 = N\sigma_p e^{-|\nu_\pm - \nu_0|/\Delta\nu}.$$

Take logarithms of both sides of equation to find:

$$\nu_+ - \nu_- = 2\Delta\nu \ln N\sigma_p.$$

Radiative forcing Q and increment ΔQ for doubling N are:

$$Q = 2\pi B_0 \Delta\nu \ln N\sigma_p, \quad \text{and} \quad \Delta Q = 2\pi B_0 \Delta\nu \ln 2 = 7.4 \text{ W m}^{-2}.$$

Numbers are $B_0 = 0.14$ **W m^{-2} str^{-1}**, $\Delta\nu = 12.2$ **cm^{-1}**. Overlap with the pure-rotational band of water vapor eliminates most of the response from the lower band edge, and IR from clouds further reduces the reponse to more CO2. The true response is likely less than half the ideal limit or:

$$\Delta Q \leq 3.7 \text{ W m}^{-2}.$$

Cross sections depend on far-wing lineshape at band edges which drive warming!

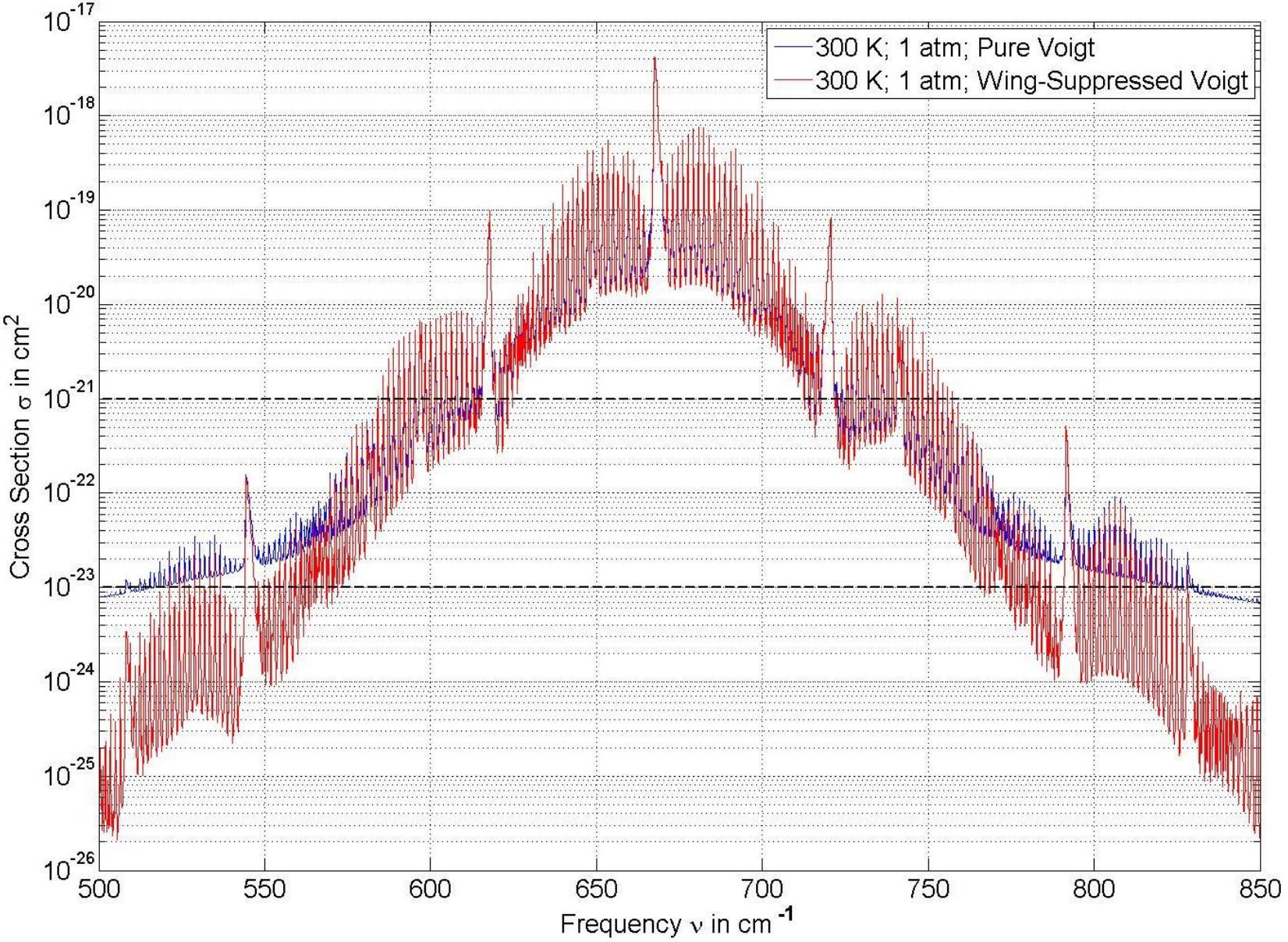

Physics Behind Shape of Emission Absorption Lines

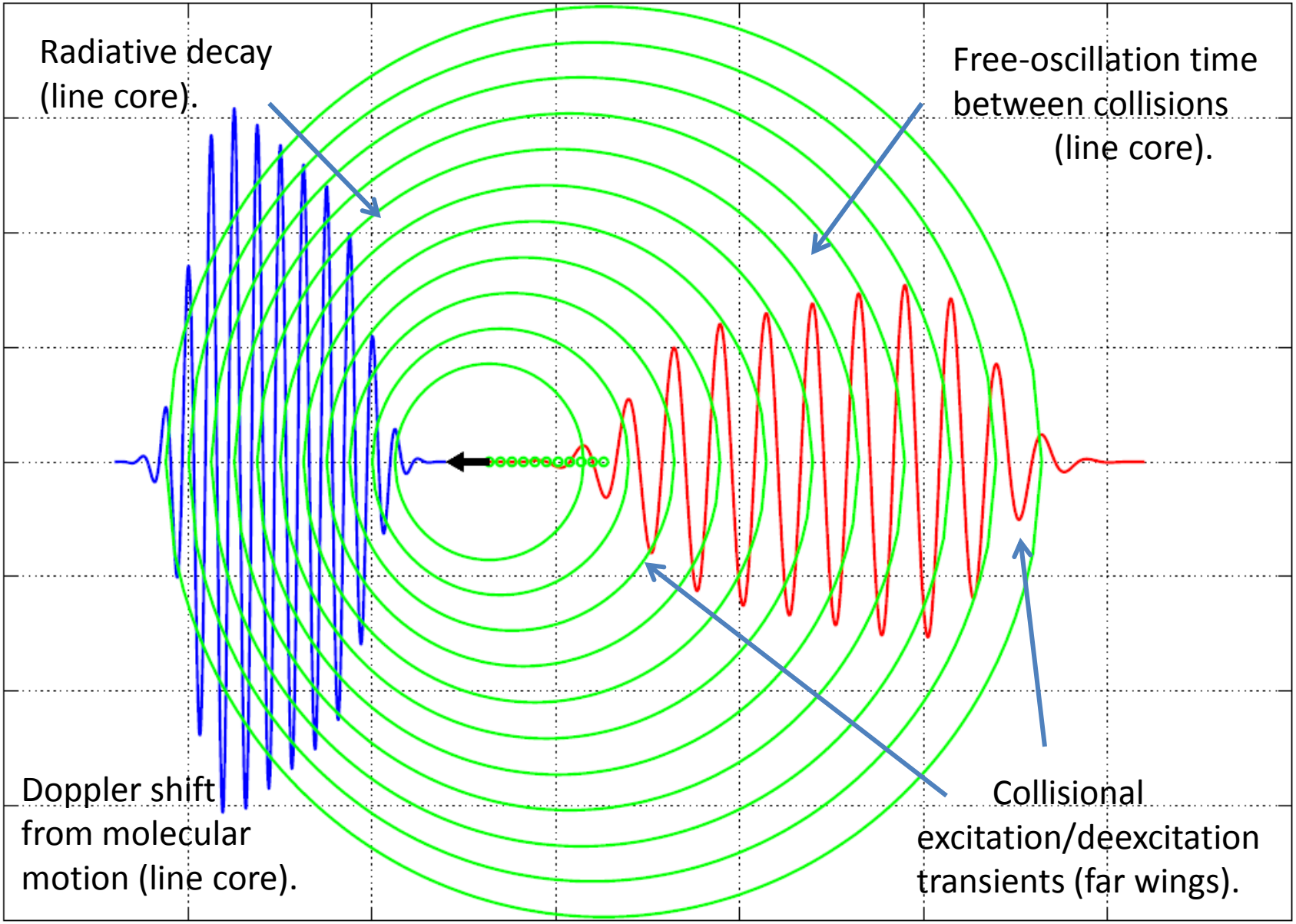

Radiation

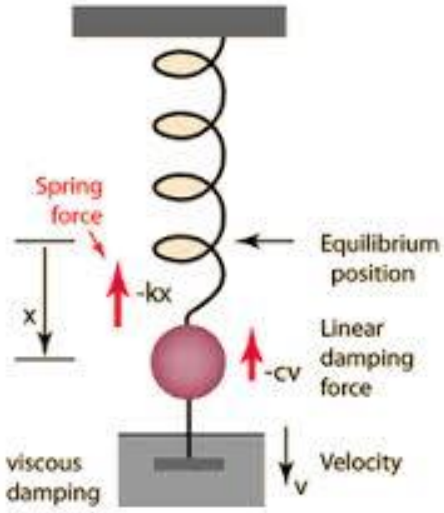

(Pre-QM Fermi's Golden Rule)

Larmor's radiated power

$$P_r = \frac{2q^2\ddot{X}^2}{3c^3} = m\tau_L\ddot{X}^2$$

Sir Joseph Larmor (1857-1942)

The Larmor time

$$\tau_L = \frac{2q^2}{3mc^3} \approx \begin{cases} 10^{-28}\ \text{s} & \text{far-infrared}\ , \\ 10^{-23}\ \text{s} & \text{far-ultraviolet}\ . \end{cases}$$

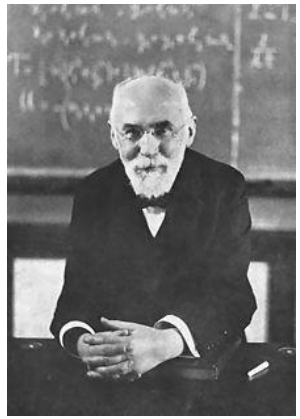

H. A. Lorentz (1853 -1928)

Viscous damping does not work as a description of radiation damping. It does not conserve energy. Radiation damping force must be proportional to the third deriviative!

The Abraham-Lorentz radiation reaction force (see Jackson's E&M for more discussion)

$$F_r = m\tau_L\dddot{X}$$

Newton's second law of motion

$$m\ddot{X} = -\kappa X + m\tau_L\dddot{X} + F$$

M. Abraham (1875 – 1922)

A Solution to Newton's Second Law, f = ma

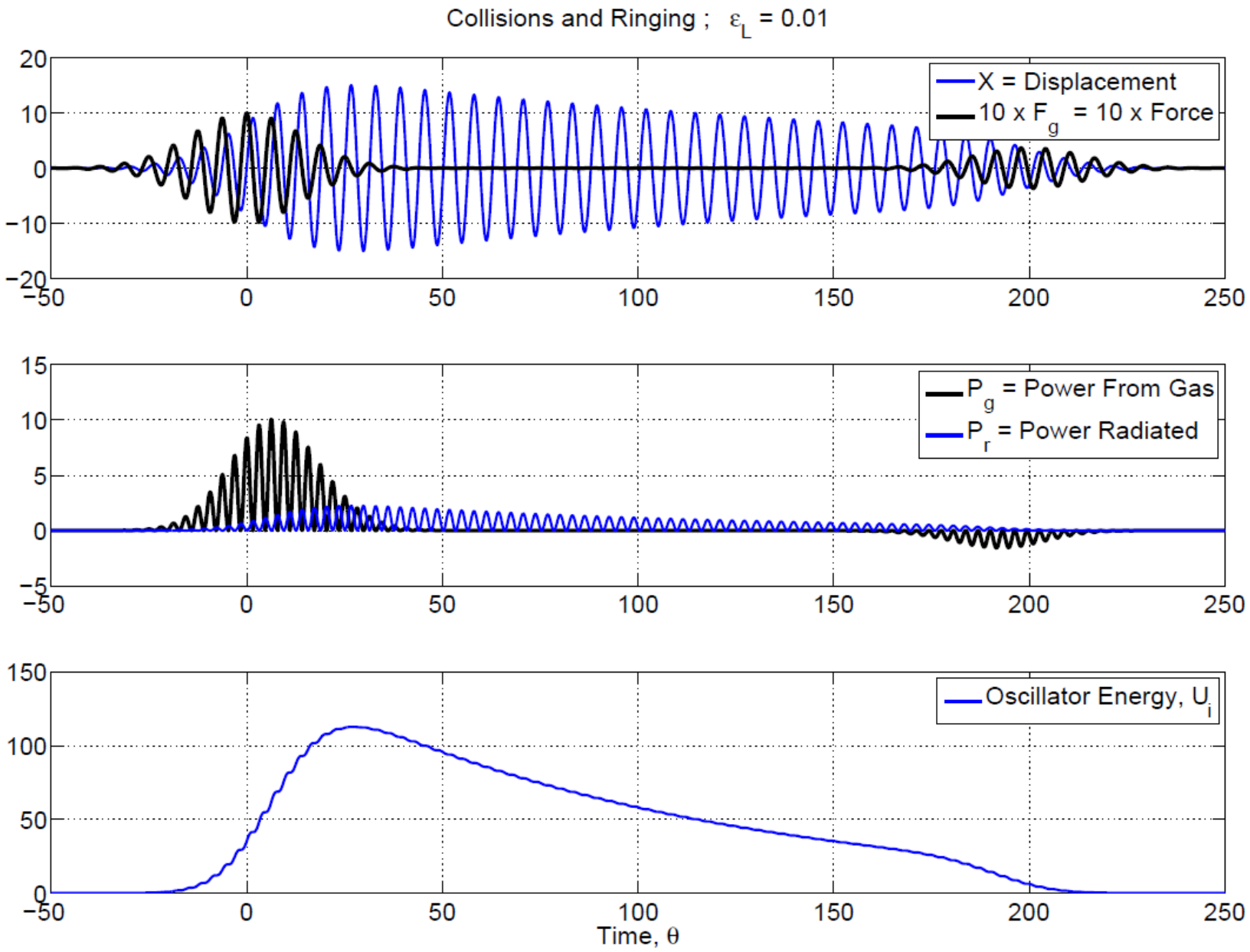

A Useful Special Function For Spectral Line Shapes

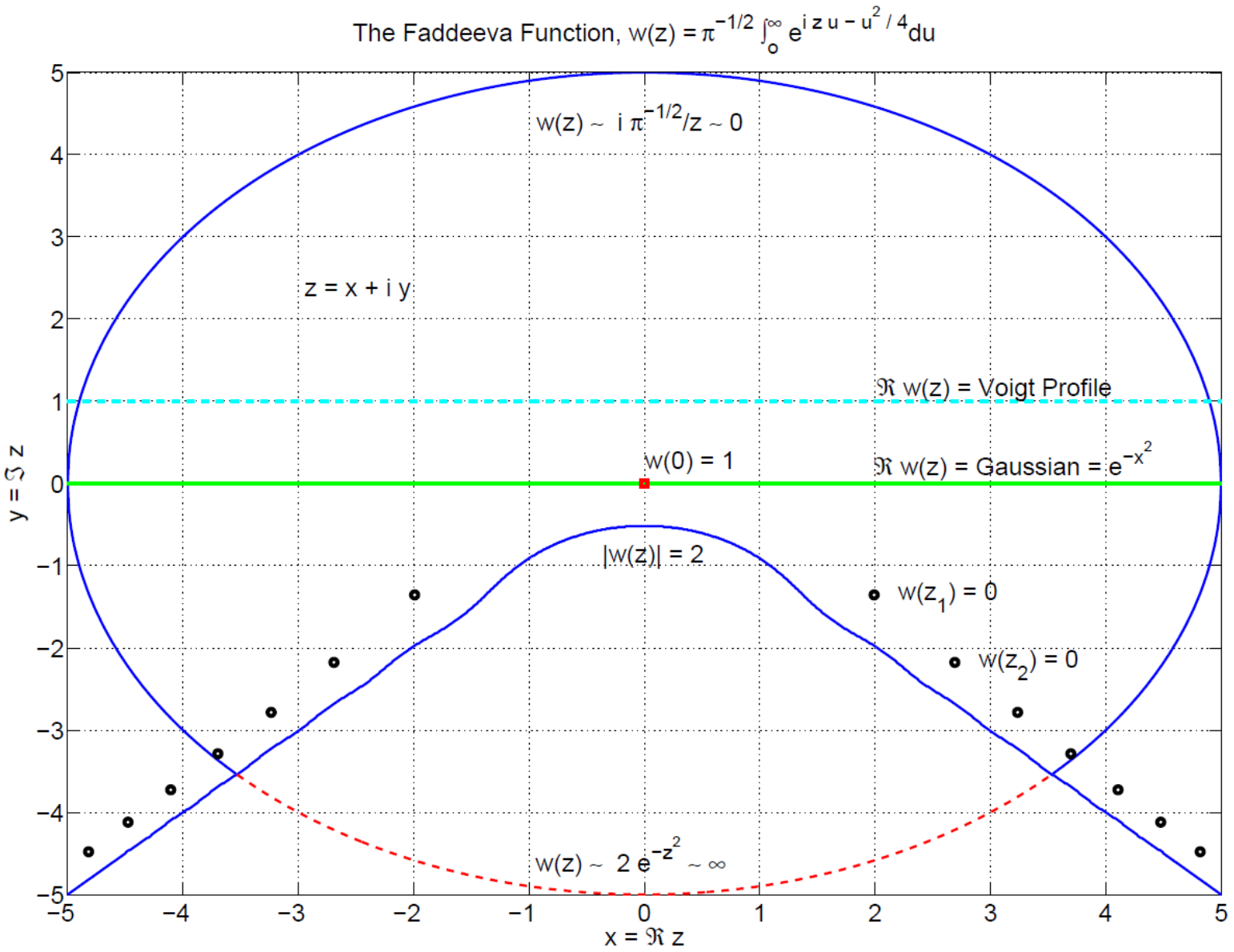

Collision-Free Cross Section (not possible with CO_2 in air) :

$$\sigma(\rho) = \frac{\rho^4}{(1-\rho^2)^2 + \epsilon_L^2 \rho^6}$$

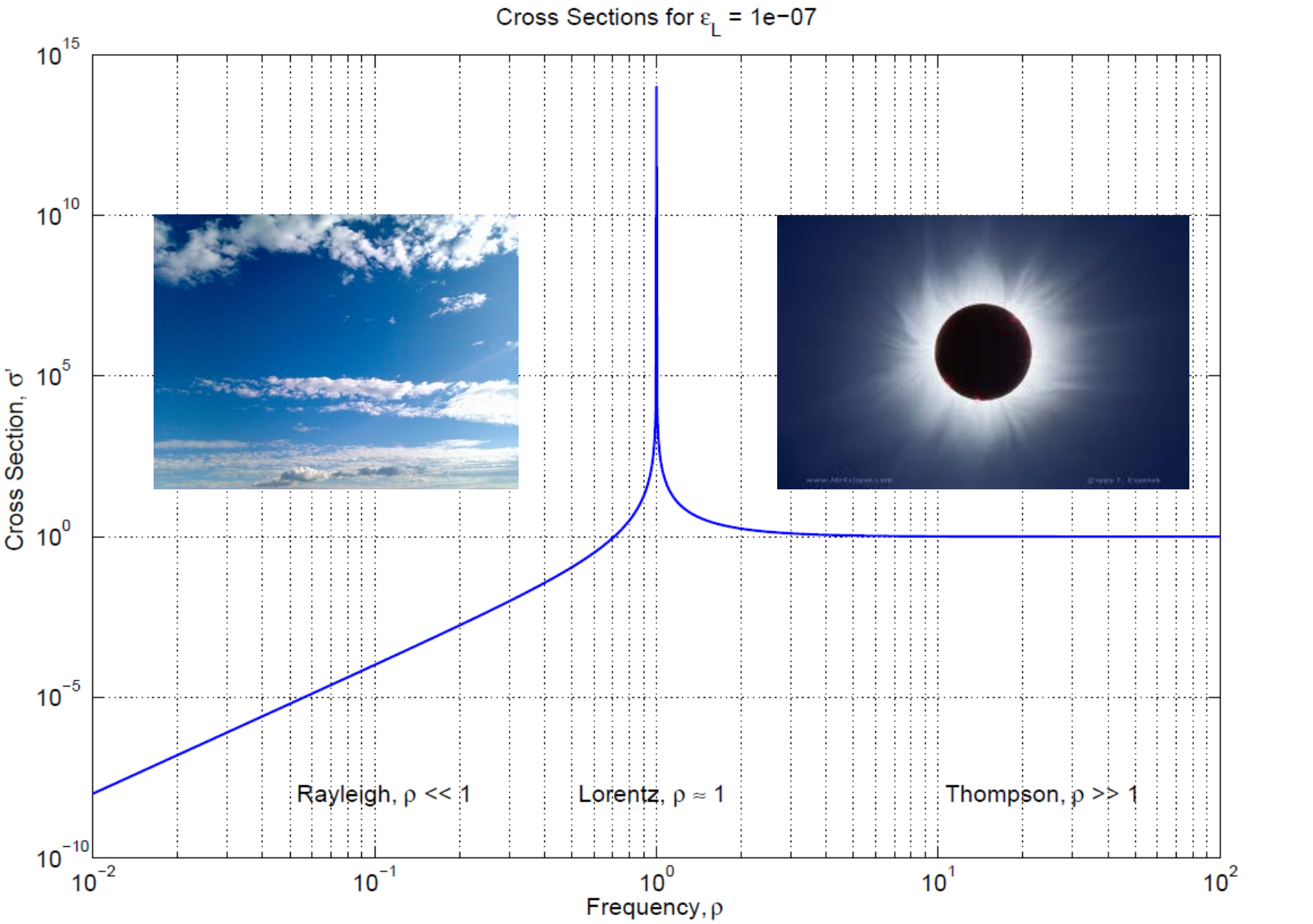

Outline of Lineshape Calculation with Collisions

$$\begin{aligned} \text{Relative time:} \quad & \theta = \omega_0 t \\ \text{Relative frequency:} \quad & \rho = \omega/\omega_0 \end{aligned}$$

$$\begin{aligned} \text{Collisional Force } F &= 2\cos(\rho_k \theta) A(\theta) \\ &= \text{carrier of frequency } \rho_k \times \text{envelope } A(\theta) \end{aligned}$$

The Fourier transform of the envelope is

$$\tilde{A}(\rho) = \int_{-\infty}^{\infty} A(\theta) e^{i\rho\theta} d\theta,$$

The resulting lineshape function is a Lorentzian, weighted by the absolute squared Fourier transform of the envelope:

$$g(\rho) = \frac{\epsilon \rho^4 |\tilde{A}(\rho - 1)|^2}{\pi\{(\rho - 1)^2 + \epsilon^2\}}.$$

$$\epsilon = \text{natural radiative broadening} + \text{collisions}$$

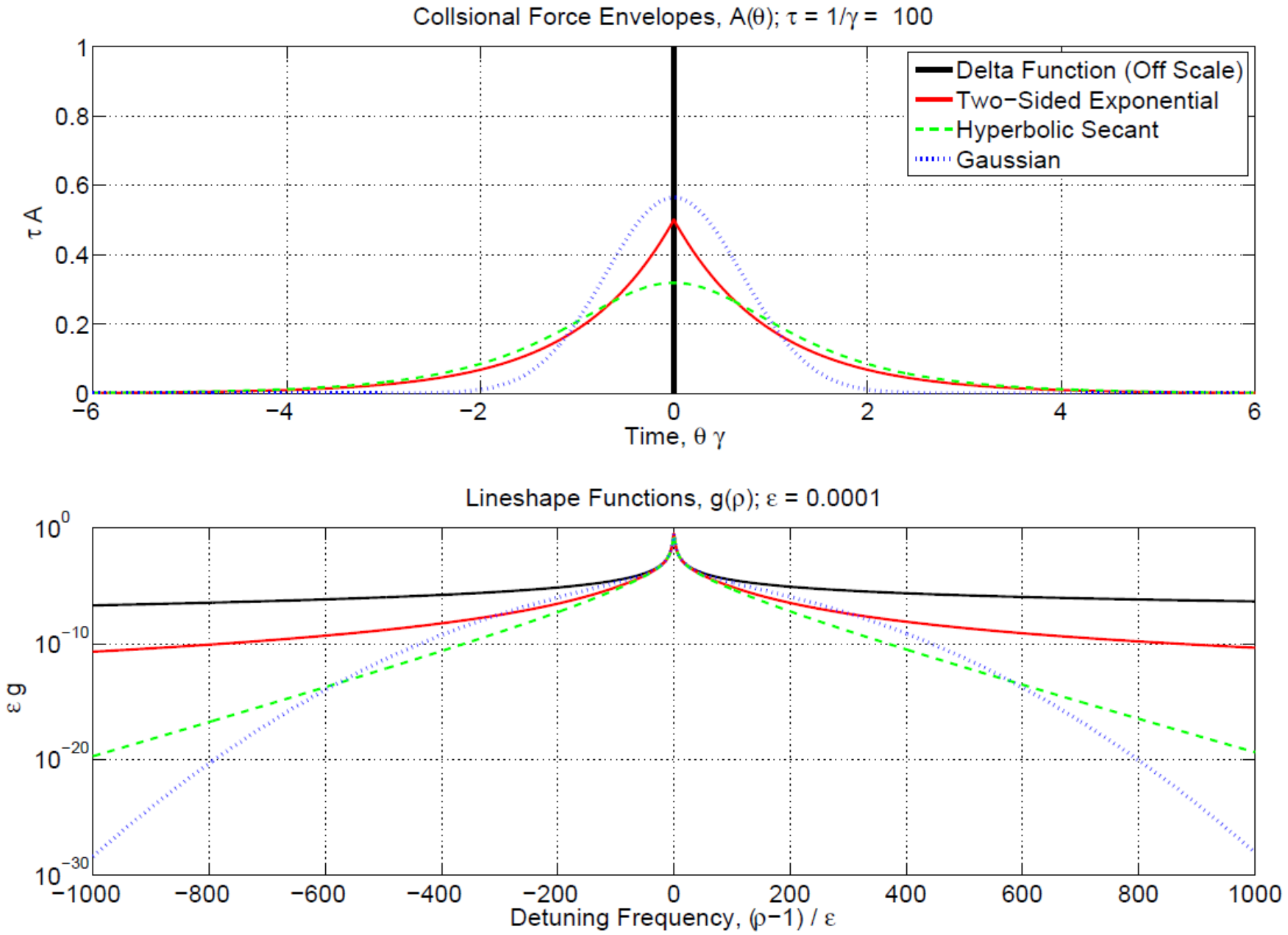
Collsional Force Envelopes, A(θ); τ = 1/γ = 100
Delta Function (Off Scale)
Two−Sided Exponential
Hyperbolic Secant
Gaussian
τ A
Time, θ γ
Lineshape Functions, g(ρ); ε = 0.0001
ε g
Detuning Frequency, (ρ−1) / ε

Far-wing (global warming) cross sections much bigger with Lorentz broadening (lines) than with realistic far-wing broadening (circles).

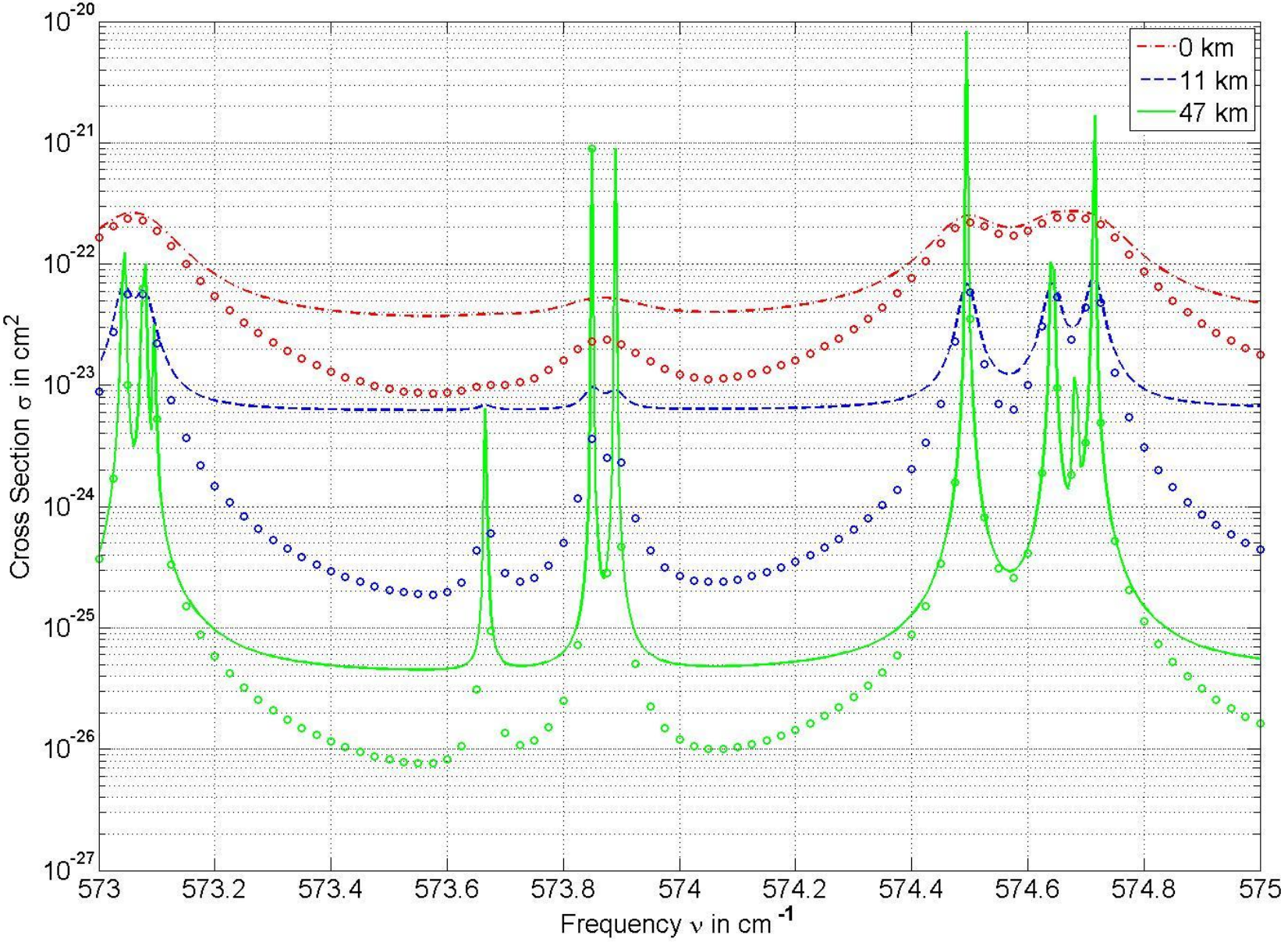

390 ppm CO_2

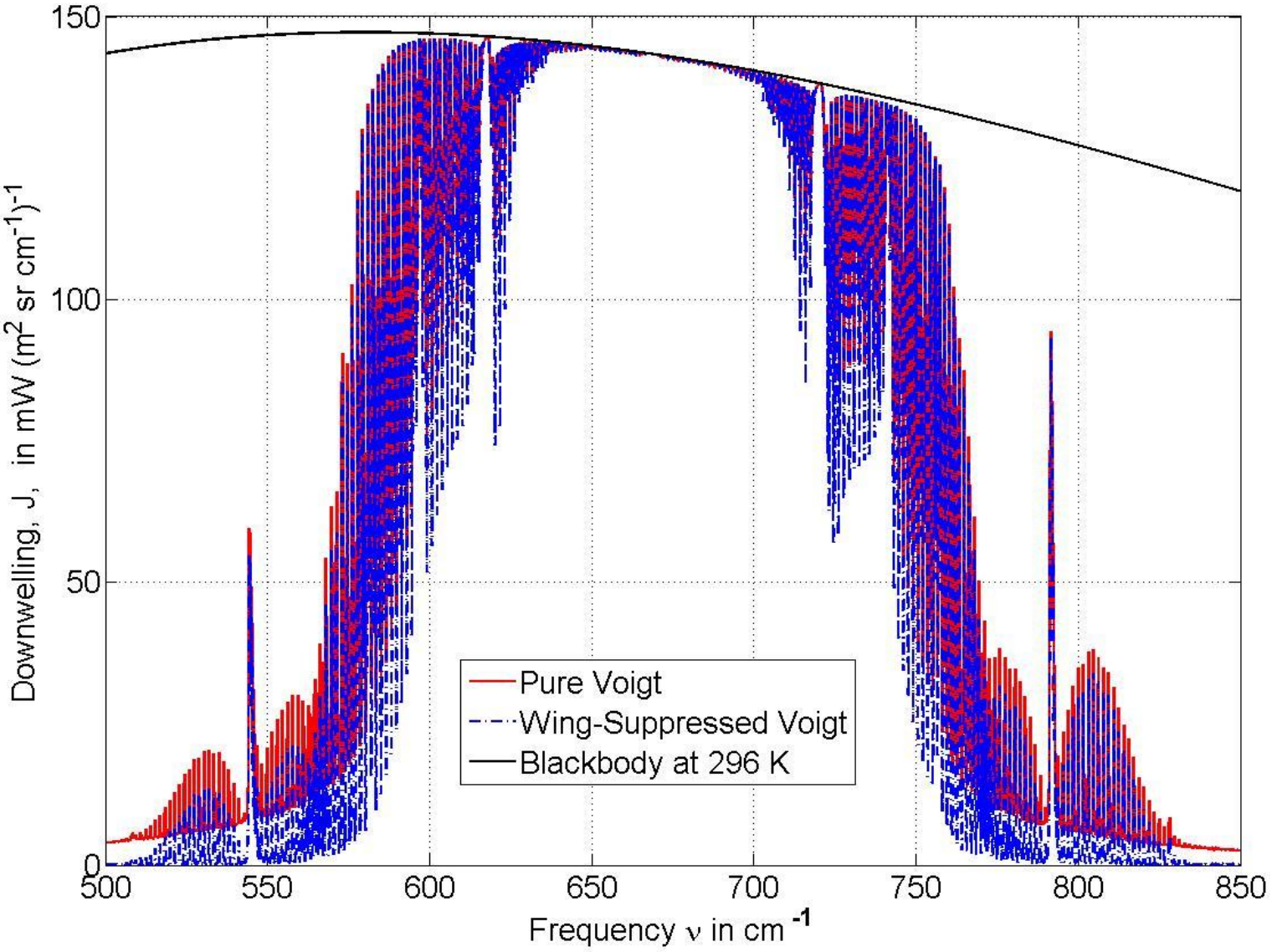
150
100
50
0
500
550
600
650
700
750
800
850
Downwelling, J, in mW (m2 sr cm-1)-1
Frequency ν in cm -1
Pure Voigt
Wing-Suppressed Voigt
Blackbody at 296 K

Using Voigt profiles increases the radiative-forcing increment from doubling CO_2 by a factor

~1.4

But far wing absorption from Voigt profiles does not exist!

Need experimental measurements!

Voigt Line Shapes Don't Work in Far Wings!

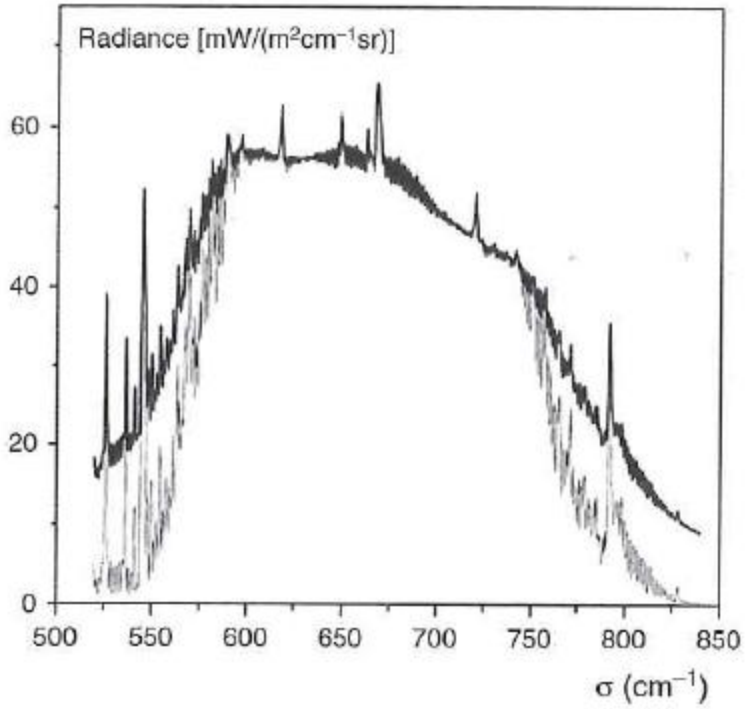

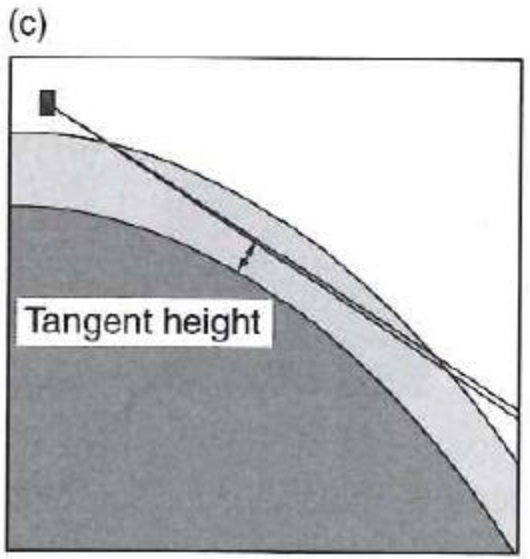

Fig. VII.15: Radiance emitted by the Earth atmosphere in the region of the ν_2 CO_2 band for a 1 cm^{-1} resolution. The thin line gives measured values obtained by a balloon-borne instrument[29] at 40 km altitude looking down to a tangent height of 10 km. The thick line corresponds to predictions using purely Voigt line shapes. After Ref. 603.

Hartmann, Boulet and Robert, *Collisional Effects on Molecular Spectra, Elsevier, 2008*

Climate models are not working! Far-wing lineshapes (forcing ΔQ_2) are one of many possible causes. Clouds (feedback f) probably even more important

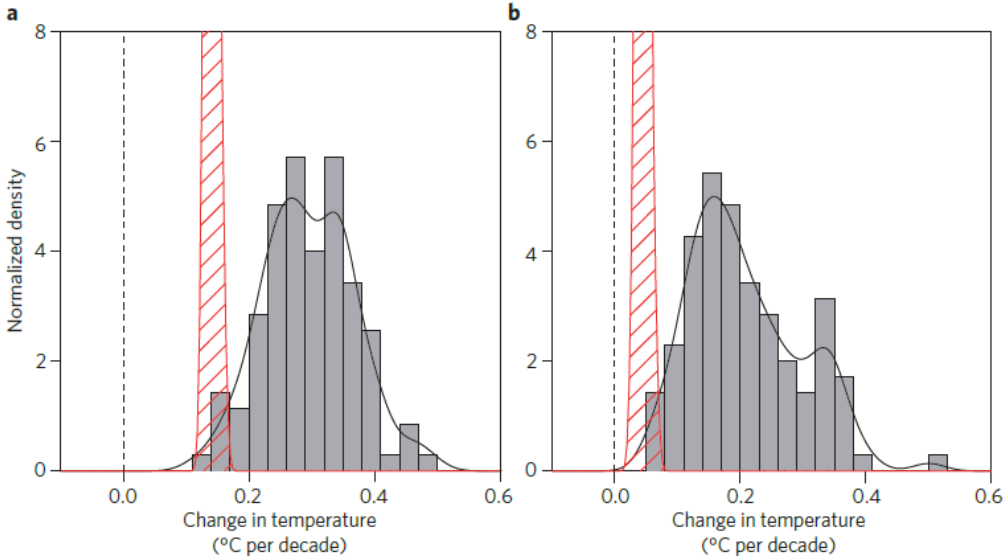

Figure 1 | Trends in global mean surface temperature. **a**, 1993–2012. **b**, 1998–2012. Histograms of

"Science is the belief in the ignorance of experts."

Richard Feynman